AGU PUBLICATIONS

JGR

Journal of Geophysical Research: Atmospheres

RESEARCH ARTICLE
10.1002/2016JD026227

Key Points:
- Oil and natural gas development was the largest source of observed VOC reactivity in the Colorado Front Range in spring 2015
- Observed VOC reactivity in the Colorado Front Range in summer 2015 was low (average = 2.4 s^{-1}) relative to other urban areas in the U.S.
- Isoprene contributed substantially to VOC reactivity in summer 2015, in contrast to a previous study

Supporting Information:
- Supporting Information S1

Correspondence to:
D. K. Farmer,
delphine.farmer@colostate.edu

Citation:
Abeleira, A., I. B. Pollack, B. Sive, Y. Zhou, E. V. Fischer, and D. K. Farmer (2017), Source characterization of volatile organic compounds in the Colorado Northern Front Range Metropolitan Area during spring and summer 2015, *J. Geophys. Res. Atmos.*, *122*, 3595–3613, doi:10.1002/2016JD026227.

Received 12 NOV 2016
Accepted 10 FEB 2017
Accepted article online 14 FEB 2017
Published online 17 MARCH 2017

Source characterization of volatile organic compounds in the Colorado Northern Front Range Metropolitan Area during spring and summer 2015

A. Abeleira[1], I. B. Pollack[1,2], B. Sive[3], Y. Zhou[2], E. V. Fischer[2], and D. K. Farmer[1]

[1]Department of Chemistry, Colorado State University, Fort Collins, Colorado, USA, [2]Department of Atmospheric Sciences, Colorado State University, Fort Collins, Colorado, USA, [3]Air Resources Division, National Park Service, Lakewood, Colorado, USA

Abstract Hourly measurements of 46 volatile organic compounds (VOCs) from the Boulder Atmospheric Observatory in Erie, CO, were collected over 16 weeks in spring and summer 2015. Average VOC reactivity (1.2 s^{-1} in spring and 2.4 s^{-1} in summer) was lower than most other U.S. urban sites. Positive matrix factorization analysis identified five VOC factors in the spring, corresponding to sources from (1) long-lived oil and natural gas (ONG-long lived), (2) short-lived oil and natural gas (ONG-short lived), (3) traffic, (4) background, and (5) secondary chemical production. In the summer, an additional biogenic factor was dominated by isoprene. While ONG-related VOCs were the single largest contributor (40–60%) to the calculated VOC reactivity with hydroxyl radicals (OH) throughout the morning in both spring and summer, the biogenic factor substantially enhanced afternoon and evening (2–10 P.M. local time) VOC reactivity (average of 21%; maxima of 49% of VOC reactivity) during summertime. These results contrast with a previous summer 2012 campaign which showed that biogenics contributed only 8% of VOC reactivity on average. The interannual differences suggest that the role of biogenic VOCs in the Colorado Northern Front Range Metropolitan Area (NFRMA) varies with environmental conditions such as drought stress. Overall, the NFRMA was more strongly influenced by ONG sources of VOCs than other urban and suburban regions in the U.S.

1. Introduction

On a global scale, biogenic emissions dominate the organic carbon budget, with anthropogenic emissions contributing <15% [*Goldstein*, 2007; *Kesselmeier and Staudt*, 1999]. Biogenic volatile organic compounds (VOCs) include isoprene and other terpenoids, as well as small oxygenated VOCs (OVOCs) and alkenes. Anthropogenic emission sources include oil and natural gas (ONG) operations (i.e., removal, refining, storage, and transport of oil or natural gas), gasoline storage and transportation, combustion (i.e., automobiles or biomass), chemical manufacturing, and solvent use [*Piccot et al.*, 1992]. However, the relative importance of anthropogenic and biogenic VOC emissions vary across regions with biogenic emissions dominating carbon mixing ratios in rural and forested regions [*Karl et al.*, 2003] and anthropogenic emissions dominating urban areas [*Baker et al.*, 2008; *Borbon et al.*, 2013; *Gilman et al.*, 2009]. Dense urban areas such as Los Angeles are dominated by automobile-related VOC emissions [*Borbon et al.*, 2013], while ONG-producing regions experience large emissions of light alkanes associated with fossil fuel extraction and refinement [e.g., *Katzenstein et al.*, 2003].

Ground-level ozone (O_3) production occurs when volatile organic compounds (VOCs) are oxidized in the presence of NO_x ($NO + NO_2$) and sunlight. The propensity of a given VOC to initiate the O_3 production cycle can be described by its reactivity with the OH radical, $R_{OH,X}$ (s^{-1}). While this parameter does not account for chain propagation or termination steps, the OH reactivity of a given species can provide insight into relative contributions of different hydrocarbons to the rate of O_3 production. The OH reactivity of a particular species is defined as the species mixing ratio in molecule cm^{-3} multiplied by its rate constant with OH

$$R_{OH,X} = k_{OH+X}[X] \quad (1)$$

The summed reactivity of all VOC species (VOC reactivity or $R_{OH,VOCs}$; s^{-1}) contributes to the total OH reactivity ($R_{OH,Total}$; s^{-1}), which includes reaction with inorganic species:

$$R_{OH,\,VOCs} = \sum_i (k_{OH+VOC_i}[VOC_i]) \quad (2)$$

$$R_{OH,\,Total} = R_{OH,NO_x} + R_{OH,CH_4} + R_{OH,CO} + R_{OH,VOCs} \quad (3)$$

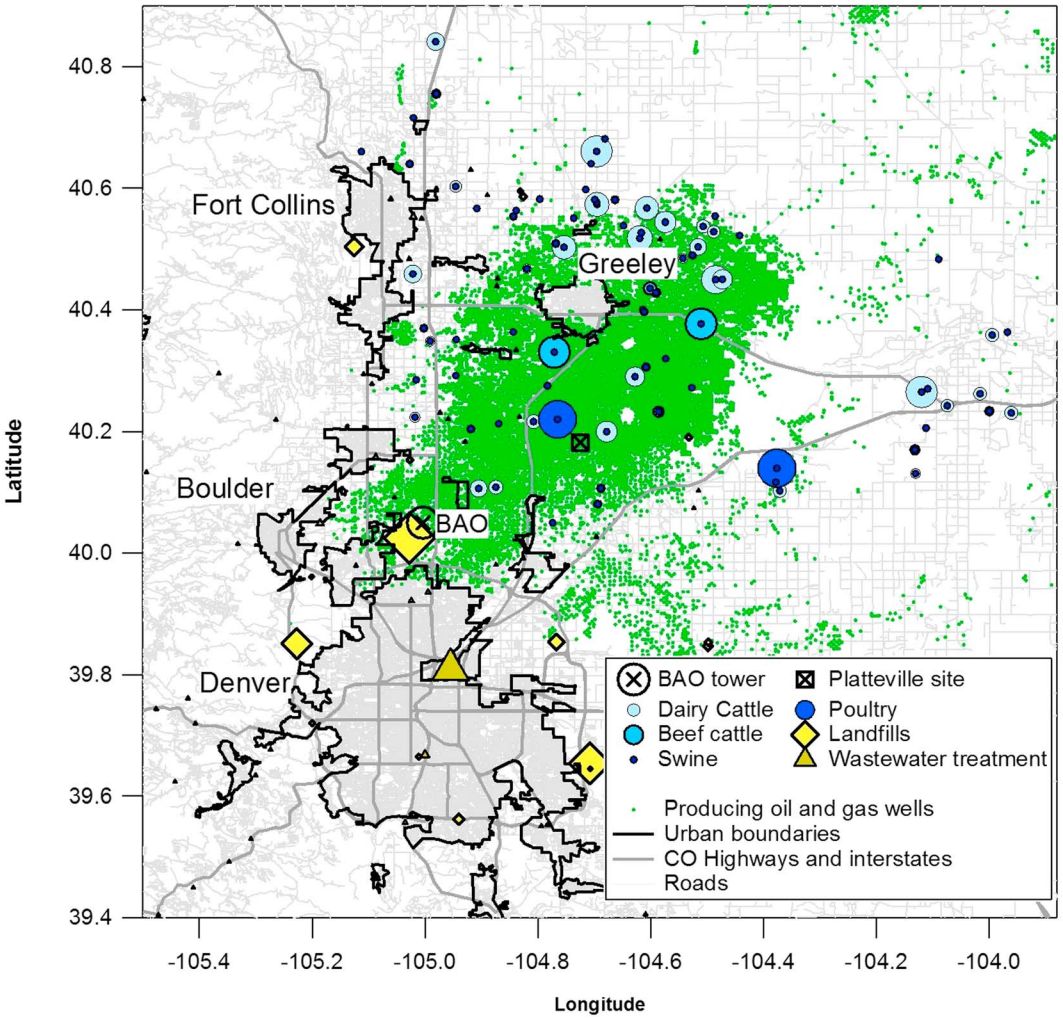

Figure 1. Major urban centers in the NFRMA include Fort Collins, Boulder, Denver, and Greeley (black outlines). The BAO site is at the SW corner of Weld County near the interface between rural and urban areas. Concentrated agriculture feed operations for beef cattle (light blue circle), poultry (dark blue circle), and dairy cattle (pale blue circle) are sized based on 2012 operation sizes. Swine operations (purple circles) are not sized. Landfills (yellow diamonds) are sized with operation size. Producing oil and gas wells as of 2012 are represented by green circles (no sizing).

These terms are typically calculated from an observed suite of VOCs. Atmospheric instrumentation quantitatively detects only a subset of VOCs. The calculated VOC and OH reactivity thus underestimates directly observed reactivity in urban, rural, and remote regions [e.g., *Chatani et al.*, 2009; *Di Carlo et al.*, 2004; *Dolgorouky et al.*, 2012; *Dusanter et al.*, 2009; *Edwards et al.*, 2013; *Hansen et al.*, 2014; *Whalley et al.*, 2016]. However, standard measurements of VOCs by gas chromatography or proton transfer reaction mass spectrometry still provide insight on the key reactivity sources at a given site.

Multiple short (<4 weeks) field campaigns have focused on understanding the primary sources contributing to VOCs in the Northern Front Range Metropolitan Area (NFRMA) of Colorado [*Brown et al.*, 2013; *Gilman et al.*, 2013; *McDuffie et al.*, 2016; *Pétron et al.*, 2012; *Swarthout et al.*, 2013; *Thompson et al.*, 2014]. This region has repeatedly exceeded the National Ambient Air Quality Standard for O_3 in the past decade and is home to a large and rapidly growing population (3.5+ million people in 2015). Repeated measurements of VOCs have been made at the Boulder Atmospheric Observatory (BAO) in Erie, CO (Figure 1). These measurements showed that the region experiences higher mixing ratios of C_2-C_6 alkanes relative to other U.S. regions, with propane, butane isomers, and pentane isomers exceeding summer time average mixing ratios in 28 other U.S. cities [*Baker et al.*, 2008]. This strong alkane source signature was highly correlated with

propane, a known marker for natural gas production [*Pétron et al*., 2012]. *Gilman et al*. [2013] reported that the majority (73–96%) of measured C_2-C_6 alkanes, and approximately half (55 ± 18%) of the calculated VOC reactivity (i.e., derived from measured VOCs via equation (2); average $R_{OH,VOC} = 3 \pm 3\ s^{-1}$), can be attributed to oil and gas production. Simultaneous and nominally colocated measurements verified the ONG source of this C_2-C_5 alkane enhancement with wind direction and back trajectory analysis showing the largest enhancements came from the Wattenberg Field natural gas production region northeast of the sampling site [*Swarthout et al*., 2013]. *Swarthout et al*. [2013] found that C_2-C_8 alkanes accounted for 61% of VOC reactivity, moreover, the C_2-C_6 alkanes, which were attributed almost exclusively to ONG activities [*Gilman et al*., 2013], accounted for 52% of VOC reactivity. Both studies also noted a second distinct VOC source related to urban combustion (i.e., tail pipe emissions or traffic sources). Enhanced tail-pipe-related VOCs (aromatics, alkenes, and ethyne) were most often associated with air mass transport from the south and west, implying sources from Denver, Boulder, and Longmont [*Swarthout et al*., 2013]. Using VOC and trace gas measurements from a summer 2012 campaign at the BAO site, *McDuffie et al*. [2016] reported an average calculated VOC reactivity of $2.4 \pm 0.9\ s^{-1}$, of which alkanes contributed 56% and biogenic VOCs contributed 8%. Measurements from Erie, Longmont, Platteville (Wattenberg Natural Gas Field), downtown Denver, and Boulder County showed higher C_2-C_5 alkane mixing ratios in residential neighborhoods near the densest drilling in the Wattenberg Natural Gas Field (Platteville) with reduced mixing ratios in areas further from drilling operations (i.e., Denver, Boulder County) [*Thompson et al*., 2014]. Correlations of benzene and toluene with ONG tracers were higher in the Platteville area relative to Denver, where vehicular tailpipe emissions dominate the benzene, toluene, and xylene sources [*Thompson et al*., 2014]. Collectively, these studies suggest that ONG and traffic sources dominate VOC reactivity in the NFRMA.

Here we describe VOC measurements collected during a lengthy campaign at the BAO site from spring and summer 2015. We evaluate seasonal variability and sources of VOCs at the BAO site using positive matrix factorization (PMF) and consider the contribution of different sources to VOC reactivity.

2. Methods

2.1. Research Site

A suite of VOCs (Tables 1 and S1 in the supporting information) and reactive trace gases (Figures S1–S3) were measured at the NOAA BAO site in Weld County. Spring measurements were made between 20 March and 17 May 2015; summer measurements were made between 5 July and 6 September 2015. The BAO site is semirural, surrounded by agricultural operations, but with growing subrban development in the town of Erie. Major urban centers are located 35 km to the south (Denver), 30 km to the west (Boulder), 65 km to the north (Fort Collins), and 65 km to the northeast (Greely) (Figure 1). A major interstate highway (I-25) runs north to south 2 km to the east of the site. The site is in the Denver-Julesberg basin on the edge of the Wattenberg natural gas field, an area of active and extensive ONG exploration and production [*Pétron et al*., 2014]. All instruments were located in air-conditioned trailers at the site. Average temperatures at the site were 10°C (range −2.5–27°C) in the spring and 24°C (range 14.5–36°C) in the summer (10 m above ground level, agl; Figure S4).

2.2. Measurements

2.2.1. Volatile Organic Compounds

An automated four-channel online gas chromatographic (GC) system was used for in situ VOC measurements. The GC system used four different separation columns and four detectors (three flame ionization detectors (FID), one electron capture detector (ECD)) to measure 46 individual VOCs (Tables 1 and S1) including C_2-C_8 nonmethane hydrocarbons (NMHCs), C_1-C_2 halocarbons, C_1-C_5 alkyl nitrates, and several OVOCs with hourly time resolution [*Sive et al*., 2005; *Zhou et al*., 2008; *Zhou et al*., 2005]. The version of the GC system deployed for this project used a cryogen-free concentration system for the online preconcentration of ambient samples that was similar to *Sive et al*. [2005] but was equipped with a different cryogen-free cooler (Q-Drive, Model 2S102K). Ambient air was collected on 1 mm silica beads at −160°C for 5 min at a flow rate of 200 mL/min for a total sample volume of 1 L. Water was removed prior to sample trapping with a higher-temperature cold trap. The GC columns used for this deployment included the following: (1) a CP-Al_2O_3/Na_2SO_4 PLOT column (50 m × 0.53 mm I.D. 10 μm film thickness; Varian, Inc.) connected to an FID

Table 1. Observed Mixing Ratios, VOC Reactivity, OH Rate Coefficients, and LODs for Select VOCs at BAO in Spring and Summer 2015[a]

	Mean Mixing Ratio (ppbv)[b]		Mean $R_{OH,VOC}$ (s^{-1})[b]				
Compound	Spring	Summer	Spring	Summer	$k_{OH,VOC}$[c]	Reference[d]	LOD (ppbv)
Ethane	16 (22)	23 (33)	0.07 (0.10)	0.1 (0.2)	0.25	a	0.008
Propane	9 (13)	8 (11)	0.2 (0.3)	0.2 (0.2)	1.09	a	0.01
i-Butane	1 (1)	2 (2)	0.04 (0.07)	0.07 (0.09)	2.1	a	0.007
n-Butane	2 (3)	4 (6)	0.1 (0.2)	0.2 (0.3	2.4	a	0.005
i-Pentane	1 (3)	3 (5)	0.1 (0.2)	0.2 (0.4)	3.6	a	0.003
n-Pentane	1 (2)	3 (5)	0.1 (0.2)	0.2 (0.4)	3.8	a	0.003
Cyclopentane	0.1 (0.1)	0.7 (1.0)	0.01 (0.01	0.1 (0.1)	5.1	b	0.004
n-Hexane	0.2 (0.3)	0.4 (0.5)	0.02 (0.03)	0.04 (0.05)	5.2	a	0.004
Cyclohexane	0.2 (0.3)	0.2 (0.2	0.03 (0.04)	0.03 (0.03)	7	a	0.02
2,3-Dimethylpentane	0.1 (0.1)	0.09 (0.09)	0.02 (0.02)	0.01 (0.01)	7	c	0.02
2-Methylhexane	0.04 (0.05)	0.09 (0.09)	0.006 (0.008)	0.01 (0.01)	7	c	0.02
3-Methylhexane	0.1 (0.2)	0.1 (0.1)	0.02 (0.03)	0.01 (0.02)	7	c	0.02
n-Heptane	0.1 (0.2)	0.1 (0.2)	0.02 (0.03)	0.02 (0.02)	6.76	a	0.01
Methylcyclohexane	0.2 (0.3)	0.2 (0.2)	0.05 (0.07)	0.04 (0.05)	9.6	a	0.02
2,2,4-Trimethylpentane	0.05 (0.07)	0.06 (0.06)	0.004 (0.004)	0.004 (0.004	3.34	a	0.02
2,2,3-Trimethylpentane	0.02 (0.03)	0.03 (0.04)	0.003 (0.005)	0.004 (0.006)	6.6	a	0.02
2-Methylheptane	0.07 (0.09)	0.04 (0.05)	0.01 (0.02)	0.008 (0.009)	9	c	0.02
3-Methylheptane	0.04 (0.05)	0.06 (0.07)	0.007 (0.010)	0.01 (0.01)	9	c	0.01
n-Octane	0.06 (0.08)	0.06 (0.07)	0.01 (0.01)	0.01 (0.01)	8.11	a	0.02
Ethene	0.04 (0.10)	0.3 (0.2)	0.01 (0.02)	0.05 (0.04)	8.5	a	0.003
Propene	0.01 (0.02)	0.05 (0.04)	0.005 (0.009)	0.03 (0.02)	26.3	a	0.01
cis-2-Butene	0.01 (0.01)	0.02 (0.03)	0.01 (0.02)	0.03 (0.04)	56.4	a	0.004
Isoprene		0.2 (0.3)		0.5 (0.5)	100	a	0.01
Benzene	0.2 (0.2)	0.2 (0.1)	0.006 (0.005)	0.004 (0.003)	1.22	a	0.03
Toluene	0.3 (0.3)	0.3 (0.2)	0.02 (0.02)	0.02 (0.02)	5.63	a	0.02
Ethylbenzene	0.03 (0.05)	0.04 (0.05)	0.005 (0.007)	0.005 (0.008)	7	a	0.01
ortho-Xylene	0.03 (0.04)	0.05 (0.05)	0.01 (0.01)	0.01 (0.01)	13.6	a	0.010
Ethyne	0.2 (0.1)	0.2 (0.2)	0.004 (0.003)	0.004 (0.003)	0.87	d	0.006
Acetaldehyde	1.2 (0.5)	1.9 (0.6)	0.3 (0.1)	0.4 (0.1)	15	a	0.08
Acetone	2.2 (0.7)	3 (1)	0.008 (0.002)	0.001 (0.004)	0.17	a	0.1
Methyl ethyl ketone	0.3 (0.2)	0.4 (0.3)	0.008 (0.004)	0.010 (0.006)	1.22	a	0.06

[a]Data for the complete suite of measured VOCs is in the supporting information (Table S1).
[b]Standard deviation of averages reported in parentheses.
[c]$k_{OH,VOC}$: $\times 10^{-12}$ cm^3 $molecule^{-1}$ s^{-1}.
[d]References for $k_{OH,VOC}$: (a) *Atkinson and Arey*, [2003] (b) *Rosen et al.* [2004], (c) *Farmer et al.* [2011], (d) *Atkinson* [1986], (e) *Sander et al.* [2015], and (f) *Atkinson et al.* [2001].

for the C_2-C_6 hydrocarbons, (2) a VF-1 ms column (60 m × 0.32 mm I.D. 1 μm film thickness, Agilent Technologies) connected to an FID for the C_{7+} hydrocarbons and aromatics, (3) a CP-PoraBond-Q column (25 m × 0.25 mm I.D. 3 μm film thickness, Agilent Technologies) coupled to an XTI-5 (30 m × 0.25 mm I.D. 0.25 μm film thickness, Restek) connected to an FID for the OVOCs, and (4) an OV-1701 column (60 m × 0.25 mm I.D. 1 μm film thickness, Ohio Valley Specialty) connected to an ECD for C_1-C_5 alkyl nitrates and C_1-C_2 halocarbons.

The VOC sampling manifold included a ¼″ O.D. perfluoroalkoxy (PFA) line (flow rate 0.2 liters per minute, LPM) with a 1 μm Teflon filter at the inlet, which was located 6 m agl. A whole air calibration standard (Cyl S; D. Blake, University of California, Irvine) with quantified levels of NMHCs, halocarbons, OVOCs, and alkyl nitrates was analyzed every tenth sampling run in the same manner as the ambient samples [*Sive et al.*, 2005] in order to monitor changes in detector sensitivity and measurement precision. Mixing ratios in the whole air standard were representative of rural air (e.g., ~400 pptv for the C_2-C_{10} NMHCs) and were similar to the cleaner air masses encountered during the campaign. This whole air standard is part of a suite of standards used with this system, which includes 10 high-pressure cylinders, 5 36 L electropolished low-pressure pontoons (~350 psi), and 3 34 L electropolished high-pressure pontoons (~900 psi) containing whole air standards (D. Blake, UC-Irvine). Calibration checks were carried out routinely for the entire suite of standards; the upper limit of the absolute accuracy of the calibrated standard is ±1–10% for the VOCs reported here.

Additional analyses were carried out in order to verify and validate the mixing ratios of the whole air working standard. The working standard was analyzed on the Colorado State University canister analytical system against one of the high-pressure pontoons, one of the low-pressure pontoons (Pont S), and one of the high-pressure cylinders (CCR24) prior to and after the SONGNEX campaign in order to ensure the standard integrity and accuracy of the mixing ratios [e.g., *Russo et al*., 2010b; *Sive et al*., 2005; *Swarthout*, 2014; *Swarthout et al*., 2013; *Zhou et al*., 2005]. The postcampaign analyses included cross-referencing to two additional standards. An additional low-pressure pontoon (PTX, D. Blake, UCI) was analyzed against the same group of standards in order to confirm consistent and comparable mixing ratios for the target gases, including the alkyl nitrates. Dilutions of a certified 1 ppmv Linde Gas NMHC multicomponent high-pressure synthetic standard were analyzed against the group of standards to further verify the calibration standards. Multipoint calibrations using primary standards evaluated the detector response and linearity over the observed mixing ratio ranges for all classes of compounds.

The measurement precision of all species were determined from replicate analysis of the whole air standard prior to deployment and were 0.6%–10% for all VOCs. Limits of detection (LODs; Table 1) were calculated as the mixing ratio required to generate a peak with a signal-to-noise ratio of 3 from replicate whole air standard analyses, where noise is defined as the standard deviation of chromatogram baseline adjacent to peaks. The LODs ranged from 2 to 23 pptv for NMHCs, $<$1 pptv to 6 pptv for C_1-C_2 halocarbons, 0.2–0.5 pptv for alkyl nitrates, and 60–100 pptv for OVOCs. Mixing ratios were calculated from adjacent points in the time series of response factors to account for variations in system sensitivity throughout the campaigns and are summarized in Table 1. The spring data set includes 1341 individual hourly samples of the full VOC suite (Table 1) minus isoprene, which was $<$ LOD during the entire spring campaign. The summer data set includes 1054 individual hourly samples of the full VOC suite (including isoprene).

2.2.2. Other Trace Gases

Peroxyacetyl nitrate (PAN) was measured with the custom-built National Center for Atmospheric Research (NCAR) GC-ECD [*Flocke et al*., 2005]. Throughout the measurement period, the LOD for PAN was 2 pptv and measurement precision was 16%. PAN was sampled through a ¼″ O.D. PFA line (flow rate ~7 LPM) with a 1 μm Teflon filter at the inlet, located 6 m agl. The total sampling line length was ~10 m from the inlet filter to the detector. PAN was produced for calibrations by photolyzing an abundance of acetone (20 ppmv) in the presence of a precisely controlled flow of NO (1 ppmv) and diluted with zero air. Point calibrations were performed every 4 h. NO and NO_2 were measured by chemiluminescence (Teledyne Model 200EU). A blue light converter (395 nm light-emitting diode (LED)-based photolytic converter; Air Quality Designs, Inc.) was placed at the inlet tip (6 m agl) to selectively convert ambient NO_2 to NO and routinely provided $>$90% conversion efficiency. The LED was switched on and off for alternating 1 min samples of NO or NO + NO_2. The NO_2 mixing ratio was determined by subtracting the ambient NO measurement from the NO detected after photolytic conversion of NO_2 to NO. CO and CH_4 were measured with a commercial Cavity Ring-Down Spectrometer (Picarro 6401). The instrument precision during the campaign was 6 and 12% for CH_4 and CO, respectively. O_3 was measured with a 2B O_3 monitor (Model 202) with a precision of 1 ppbv over a range of 0–100 ppmv when calibrated with the 2B O_3 source (Model 306).

2.2.3. Data Treatment

All trace gas measurements were aligned with the hourly VOC measurements by averaging the measurement values that fell within ± 2 min of the VOC timestamps to encompass the 5 min VOC sampling window. Eighteen days were significantly impacted by smoke transported from wildfires in the western U.S. as indicated by elevated CO. These data were excluded for the analysis herein, resulting in 512 time points (24 July 2015 to 14 August 2015) of overlapping VOC and trace gas data for a "smoke-free" summer campaign data set.

2.3. Positive Matrix Factorization (PMF)

Source apportionment techniques are statistical analysis approaches used to separate ambient mixing ratios of multiple species into factors that covary simultaneously, thus representing direct sources of species, chemical processes affecting those species, or transport processes [e.g., *Guha et al*., 2015; *Lanz et al*., 2007; *Lee et al*., 1999; *Paatero*, 2000; *Paatero and Tapper*, 1994; *Song et al*., 2006; *Ulbrich et al*., 2009; *Watson et al*., 2001]. Positive matrix factorization (PMF) is an algorithm for solving a source-receptor model that assumes that species in a measured data set adhere to a mass-balance for a number of source profiles with varying

contributions to each species over the duration of the data set [*Hopke*, 2000; *Paatero*, 2000; *Paatero and Tapper*, 1994; *Ulbrich et al*., 2009]. PMF has been widely used as a source apportionment technique for aerosols [e.g., *Lanz et al*., 2007; *Lee et al*., 1999; *Song et al*., 2006; *Ulbrich et al*., 2009] and VOCs [e.g., *Bon et al*., 2011; *Guha et al*., 2015; *Yuan et al*., 2012].

For a PMF analysis, data are arranged in a $m \times n$ two-dimensional matrix (X). In equation (4), X_{ij} represents an element of the matrix X that will be fit, where the matrix columns (j) are individual VOC species, and the rows (i) are measured VOC mixing ratios. A second matrix containing the errors for each data point is also required for the PMF algorithm to weight the importance of any data point based on the uncertainty reported in that data point. Errors for each VOC data point are defined below (section 2.3.1).

$$X_{ij} = \sum\nolimits_p g_{ip} f_{pj} + e_{ij} \tag{4}$$

The PMF algorithm solves the model with positively constrained factor values (p); each factor has a single time series and factor contribution profile for each VOC included in the input matrix. Moreover, in equation (4), g_{ip} represents an element of the factor time series matrix (G), in which columns are individual factor time series; f_{pj} represents an element of the factor profile matrix (F), in which rows are the individual factor profiles; e_{ij} represents an element of the residuals matrix (E) for data points not fully fit by the selected number of factors.

The PMF algorithm uses a least squares method to iteratively fit values of the G and F matrices to minimize a quality of fit parameter Q, defined in equation (5) as

$$Q = \sum\nolimits_{i=1}^{m} \sum\nolimits_{j=1}^{n} \left(\frac{e_{ij}}{\sigma_{ij}} \right)^2 \tag{5}$$

where σ_{ij} is an element of the $m \times n$ matrix of estimated errors of the points in the data matrix. In equation (4), Q is the sum of the squares of the scaled residuals, where the scaling factor is the given error value of the data point being fit. A theoretical value of Q, or "*Q Expected*" (Q_{exp}), is equal to the degrees of freedom of the fitted data:

$$Q_{exp} = mn - p(m + n) \tag{6}$$

If the estimation of errors in the input error matrix accurately describes the true error in the measurements, then Q_{exp} should approximate Q, and Q/Q_{exp} should approach 1 with the appropriate number of factors.

The PMF user must select the appropriate number of factors that best explains the variability in the data set without including so many factors that spurious "factor splitting" occurs [*Ulbrich et al*., 2009]. This is accomplished by using the Q/Q_{exp} value as a metric for the "goodness" of fit and by evaluating how well each species is reconstructed by the chosen number of factors. Factor splitting occurs when too many factors are included and real, physically relevant factors (sources) are separated into multiple unrealistic factors (sources). A priori information regarding the number of factors/sources and the identity of those factors/sources is not required for PMF analysis, but prior knowledge of potential sources provides the user with real physical constraints upon which to base the factor number selection.

Here we applied PMF to the spring and summer data sets to investigate VOC sources and chemical processes in the NFRMA (bilinear model solved with the PMF2 algorithm in robust mode; PMF output was evaluated using the PMF evaluation tool [*Ulbrich et al*., 2009]). The ratio of Q/Q_{exp} and FPEAK are two parameters commonly included in the PMF literature to describe the factor solutions [*Hopke*, 2000; *Paatero*, 2000; *Paatero and Tapper*, 1994; *Ulbrich et al*., 2009]. For the spring VOC data set, we selected a five-factor solution with $Q/Q_{\mathrm{exp}} = 2.51$ at FPEAK = 1. For the summer data set, we selected a six-factor solution with $Q/Q_{\mathrm{exp}} = 5.87$ at FPEAK = 1. Exploration and investigation of Q/Q_{exp} and FPEAK are described in the supporting information. The additional summer factor was required to accurately explain the summer isoprene mixing ratios, which had a unique diel cycle relative to other VOCs, but contributes substantially to OH reactivity (see section 3.4). We evaluate the two seasonal solutions and compare VOC sources in spring versus summer. Solutions with more than five factors for the spring solution (or six for the summer) yielded uninterpretable factors, likely the result of the splitting of physically meaningful factors into multiple meaningless factors [*Bon et al*., 2011; *Lee et al*., 1999; *Ulbrich et al*., 2009].

2.3.1. PMF Data Preparation

We applied the PMF analysis separately for the VOC data for spring and summer, and interpreted the resulting factors with other trace gas measurements. Missing time points for each VOC species are due to unclear or indiscernible chromatograms, and were thus deemed to be below the LOD. The statistics for ethene and propene are provided in Table 1 for summer but not spring because the summer chromatographs contained reliable peaks for those two compounds while the spring measurement did not. However, in order to be able to directly compare spring and summer PMF factors, we left them out of the PMF analysis. Such points were replaced with the relevant LOD divided by 3, and the error associated with that point was assigned a value equal to the LOD in order to reduce the weight of that point in the PMF algorithm. Each species time series was scaled to obtain a campaign median value for each species of 1. This scaling provides a consistent range of values to represent species that typically vary over orders of magnitude and improves the visualization of the PMF output plots in order to improve the ease in interpretation. This does not affect the interpretation of the PMF results because the PMF algorithm explores covariability among species in the input matrix, which is independent of the actual magnitude of each species. The error matrices were generated using the relative standard deviation (RSD) of the whole air standard time series instead of the reported replicate measurement precision. This approach to errors yielded satisfactory Q/Q_{exp} values and better species reconstructions than other methods, yet represents physical uncertainty in the VOC measurements. Variations on scaling methods, error estimation, and missing data handling exist but are similar to the procedures used herein [*Bon et al*., 2011; *Guha et al*., 2015; *Hopke*, 2000; *Williams et al*., 2010; *Yuan et al*., 2012].

We estimated the uncertainty for each factor time series (Figures S5 and S6) and factor profiles (Figures 2a and 2b) using 1000 bootstrapping runs for each season [*Ulbrich et al*., 2009]. Bootstrap data sets are constructed from randomly sampled blocks of observations of varying length from the original data set matrix for the user specified number of factors. The PMF output of the sampled blocks is averaged with the standard deviations providing an error estimate for the chosen PMF solution [*Environmental Protection Agency*, 2014].

3. Results and Discussion

3.1. VOC Mixing Ratios: Seasonality and Context

Similar to previous studies in the NFRMA [*Gilman et al*., 2013; *Pétron et al*., 2012; *Swarthout et al*., 2013; *Thompson et al*., 2014], the values presented in Table 1 indicate that we observed higher mixing ratios of C_2-C_6 alkanes relative to 28 cities and urban areas in the U.S. [*Baker et al*., 2008]. For example, typical urban U.S. sites show summer daytime propane mixing ratios of 0.29– 3.51 ppbv, with Los Angeles exhibiting propane mixing ratios up to 6.05 ppbv [*Baker et al*., 2008]. In contrast, the summer NFRMA average mixing ratio of propane was 8 ppbv. However, these mixing ratios are generally lower than observed in the Marcellus Shale natural gas producing region of southwest Pennsylvania, where propane averaged 13 ppbv at a site close to a cluster of unconventional natural gas wells [*Swarthout et al*., 2015]. Propane is not the only elevated light alkane in the NFRMA: average daytime summer n-butane and n-pentane mixing ratios in this study were 2 and 1 ppbv, respectively. These observations are consistent with a strong contribution of ONG activities to the VOCs in air masses impacting the BAO site relative to urban areas in the U.S, but with lower mixing ratios of ONG-linked hydrocarbons than reported by for the Marcellus shale sites adjacent to wells [*Swarthout et al*., 2015].

Most of the average VOC mixing ratios exhibited marked changes between the spring and summer campaigns (Table 1). VOCs in urban regions often reach maxima during winter months resulting from decreased photochemistry and shallower, more stable boundary layers [*Russo et al*., 2010b]. However, at the BAO site, average mixing ratios of C_4-C_6 alkanes were typically higher in the summer than in the spring; butane doubled between the seasons, while pentane mixing ratios increased by a factor of 3. These observations are similar to previous studies in New England [*Russo et al*., 2010b] and San Paulo, Brazil [*Dominutti et al*., 2016], which attributed the seasonality to enhanced evaporative emissions with increased temperature. The other notable exception to the pattern of higher VOC mixing ratios in the spring versus summer was isoprene, which was below the detection limit in the spring but observable in the summer, consistent with isoprene's known temperature- and light-dependent biogenic source.

Repeated measurements of VOCs have been made at BAO; however, the short nature of the campaigns and differences in measurement time periods limits our ability to make quantitative comparisons between past

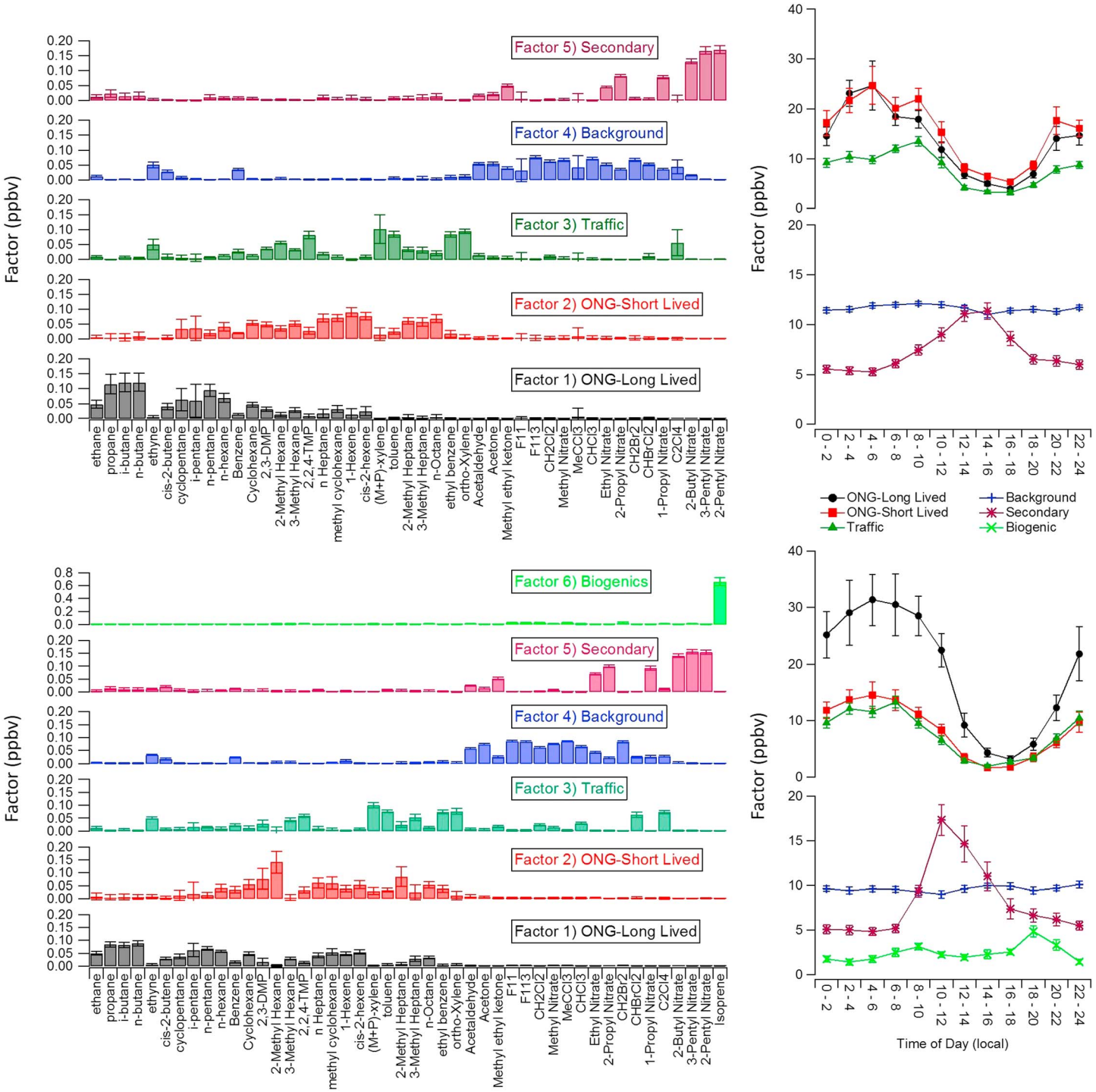

Figure 2. PMF VOC factor profiles for (a) spring and (b) summer were generated from 1000 bootstrapping PMF runs. The *y* axis for each factor profile is the fractional contribution that each species makes to each factor; error bars represent one standard deviation from the mean of the bootstrapping runs. The PMF algorithm generates an hourly time series of each factor (Figures S5 and S6). Diel cycles (ppbv) were calculated from those time series for 2 h time bins in (c, d) spring and (e, f) summer. Error bars represent the standard error of the mean (spring $n = 90–130$; summer $n = 37–48$) for each time bin average. Isoprene was measured only in the warmer summer months (average of 0.200 ppbv), dominating a sixth Biogenic PMF factor in the summer. Abbreviated compound names: 2,3-DMP = 2,3-dimethylpentane; 2,2,4-TMP = 2,2,4-trimethylpentane.

data and the 2015 data sets. Changes in ambient VOC mixing ratios could be due to a number of factors including changes in local emissions from regulatory action, well number or production, background VOC abundances [e.g., *Helmig et al*., 2016], traffic patterns, local industrial practices, synoptic scale transport, and local meteorology. Average 2015 spring C_2-C_5 alkane and ethyne mixing ratios from this study were lower than those reported by *Swarthout et al*. [2013] and *Gilman et al*. [2013] for the previous (18 February 2011–14 March 2011) Nitrogen, Aerosol Composition, and Halogens on a Tall Tower (NACHTT) campaign at BAO. Benzene and toluene mixing ratios were similar in spring 2015 to measurements from the NACHTT 2011 campaign. Some species were also lower in summer 2015 (8 week average) relative to summer 2012 (14 day average) [*McDuffie et al*., 2016]. For example, propane and n-butane were higher in summer 2012 (14 and 6 ppbv averages, respectively) [*McDuffie et al*., 2016] than summer 2015 (8 and 4 ppbv). However, this trend was not universal across the hydrocarbons: i-pentane and n-pentane were higher in summer 2015 (3 ppbv for both) than summer 2012 (2 ppbv for both) [*McDuffie et al*., 2016]. Direct comparison of average mixing ratios between the two campaigns is currently qualitative at best, and a more comprehensive comparative analysis is beyond the scope of this paper.

3.2. PMF Factors

The PMF analysis discussed here describes the VOC sources in the NFRMA (Figure 2), as observed at the BAO site in spring and summer 2015. Five factors were identified for the spring VOC data set, which are described as the following: (1) ONG-long lived, (2) ONG-short lived, (3) traffic, (4) background, and (5) secondary. A sixth factor was identified for the summer VOC data set, (6) biogenics (Figure 2). PMF assumes no loss or production processes occur between the emission point and measurement location, but in reality that is not the case. These factors are not complete representations of sources and are limited in that they do not capture the loss of highly reactive species, dry deposition processes, or gas-particle partitioning, but nonetheless, the groupings in these factors provide useful information regarding local emissions. CO, NO_x, and CH_4 were left out of the PMF analysis in order to be used as emission tracers to aid in characterizing the PMF output. That is, if all the trace gas data is incorporated in the PMF analysis, there is no remaining tracers with which to independently identify or validate factors.

Two factors were consistent with ONG-related hydrocarbons, one dominated by higher-reactivity alkanes ("ONG-short lived") and one dominated by lower-reactivity species ("ONG-long lived"). The ONG-long lived factor accounted for 36–100% of the observed C_2-C_6 alkane mixing ratios and is similar to percentages attributed to unconventional natural gas operations in the Marcellus Shale producing region of Pennsylvania [*Swarthout et al*., 2015]. Previous studies have attributed the elevated C_2-C_6 alkane mixing ratios in the NFRMA to regional ONG operations [*Gilman et al*., 2013; *Pétron et al*., 2012; *Swarthout et al*., 2013; *Thompson et al*., 2014]. The ONG-long lived factor was the sole source of propane, reconstructing 100% of the measured propane mixing ratios for both spring and summer (r^2 of 0.96 for both seasons). ONG activity is thought to be the dominant source of propane in the NFRMA [*Gilman et al*., 2013; *Swarthout et al*., 2013], which is consistent with this factor assignment, and it is unlikely that other anthropogenic sources would contribute such high mixing ratios of propane in this region. The propane-to-ethyne emission ratio normalized to volume of fuel consumed in vehicle exhaust is typically <0.1 [*Fraser et al*., 1998], in contrast to the observed propane-to-ethyne ratios of 45 and 40 for spring and summer, respectively. While emission ratios normalized to fuel consumption will not be identical to the observed ratio, the comparison supports the conclusion that combustion was not the dominant source of propane.

The ONG-short lived factor was dominated by larger C_7 and C_8 alkanes (e.g., 2-methylhexane, 2-methylheptane, and n-octane). These alkanes are known ONG emissions; for example, flashing from oil and condensate tanks emits VOCs enriched in C_7 and larger alkanes [*Berger and Anderson*, 1981; *Warneke et al*., 2014]. While this ONG-short lived factor does not contain the propane expected in an ONG source, the ONG-long lived and ONG-short lived factors share temporal characteristics indicative of a common source, with high correlation coefficients between ONG-long lived and ONG-short lived factors ($r^2 = 0.62$ and 0.63 for spring and summer, respectively; Figure S7). However, the factors are distinguished by their photochemical lifetimes. The C_2-C_5 alkanes that dominate the ONG-long lived factor have rate constants with OH on the order of $(0.25–4) \times 10^{-12}$ cm^3 molecule^{-1} s^{-1}, while the C_7-C_8 alkanes that dominate the ONG-short lived factor have faster rate constants with OH of $(7–10) \times 10^{-12}$ cm^3 molecule^{-1} s^{-1} (Table 1). These faster rate constants cause the larger alkanes to be removed 2–40 times faster than their smaller counterparts and thus to have shorter atmospheric lifetimes than the C_2-C_5 alkanes. This is consistent with *Yuan et al*. [2012],

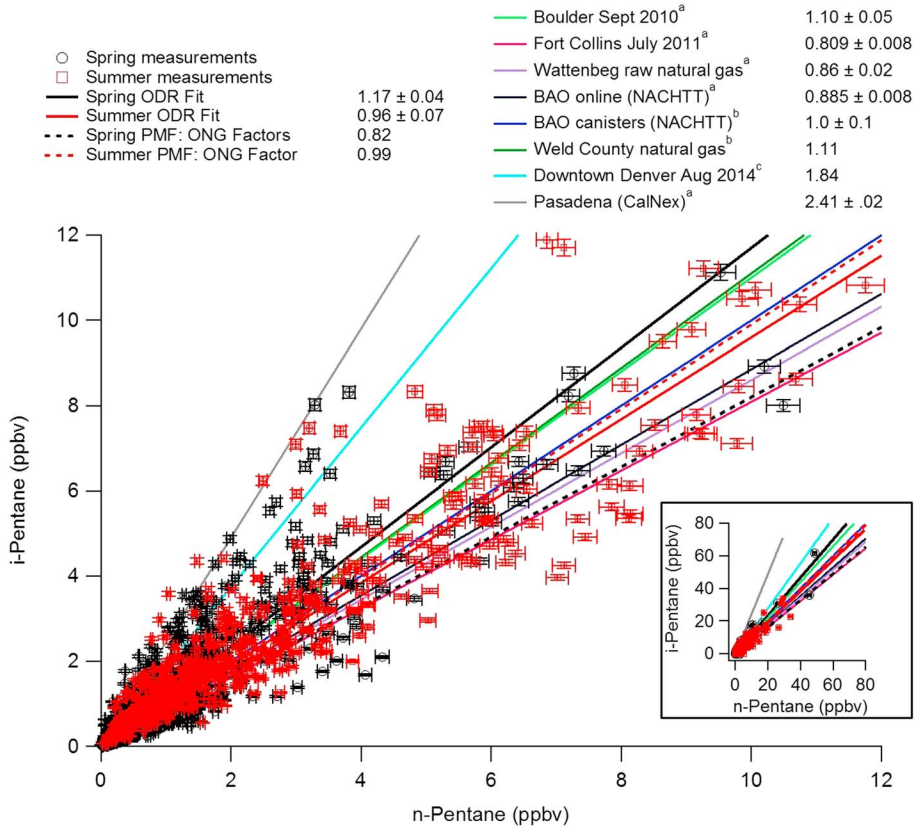

Figure 3. The ratio of i-pentane to n-pentane is used as a tracer for the relative influence of oil and natural gas production versus traffic sources. Black circles (red squares) are hourly spring (summer) measurements of i-pentane and n-pentane from the 2015 campaign. Error bars represent the uncertainty in each measurement. The solid black (red) line is the slope for spring (summer) data from an orthogonal distance regression. The dashed red and black lines represent the i-pentane/n-pentane ratios generated from the summed short + long lived ONG PMF factor profiles. The remaining solid lines are i-pentane/n-pentane ratios from previous NFRMA studies (Boulder 2010, Fort Collins 2011, BAO 2011, downtown Denver 2014), raw natural gas samples from the Wattenberg natural gas field and Weld County Natural gas in NFRMA, and the CalNex 2010 campaign in Pasadena, CA. Citations: (a) *Gilman et al.* [2013], (b) *Swarthout et al.* [2013], and (c) B. Sive (unpublished data, 2014).

which showed "chemical splitting" of a single source resulted in multiple factors separated by photochemical lifetime. Further evidence for chemical splitting of the ONG factors lies in i-pentane/n-pentane ratios. The individual factors have different pentane isomer ratios that do not represent typical ONG VOC composition but summing the two ONG factors results in i-pentane/n-pentane ratios of 0.82 and 0.99 for spring and summer, respectively. These ratios are consistent with the i-pentane/n-pentane ratio range of natural gas from NFRMA sources (1.11 for Weld County natural gas [*Swarthout et al.*, 2013] and 0.86 for Wattenberg basin raw natural gas [*Gilman et al.*, 2013]). The traffic PMF factor has an i-pentane/n-pentane ratio < 1.0, much lower than the ratios typical of combustion emissions (e.g., 2.45, for traffic dominated VOCs in the Los Angeles tunnel study [*Fraser et al.*, 1998]). This discrepancy may be the result of colocation of vehicle and ONG emissions that are not separated by the PMF algorithm and cause larger residuals for the pentane isomers resulting in poorer factor separation.

Figure 3 highlights the potential impact of these sources on the ambient VOC mixture. The ONG factors dominated the ambient pentane isomer levels at BAO in 2015 accounting for 58–63% of pentane isomers in spring and summer. The observed spring 2015 i-pentane/n-pentane ratio (1.17) was slightly higher than previous observations at BAO and other NFRMA measurements. NACHTT 2011 (winter/spring) measurements yielded i-pentane/n-pentane ratios of 0.89 [*Gilman et al.*, 2013] and 1.0 [*Swarthout et al.*, 2013]. The increased ratio could be due to one or a combination of changing background VOC mixing ratios, decreasing ONG VOC emissions as a result of regulation [*Colorado Department of Public Health and Environment*, 2014], changes

in oil and gas production in the NFRMA [*U.S. Energy Information Administration*, 2016a, 2016b, 2016c], increased traffic emissions from increased NFRMA population (14% increase in Denver county population between 2010 and 2015 [*U.S.-Census*, 2016]), or differences in meteorology and circulation that would draw air masses from areas in the NFRMA with different emissions (e.g., downtown Denver versus northeast NFRMA). Figure 3 contrasts the observed i-pentane/n-pentane ratios with other sites. The ratios in the NFRMA outside of downtown Denver were still lower than those observed in Pasadena (2.41) or Houston (1.39 [*Gilman et al*., 2009]), suggesting that the relative contribution of ONG and traffic to pentane in the NFRMA was still more weighted toward ONG than for other U.S. cities.

The third PMF factor (traffic) described traffic-related VOCs and was dominated by ethyne, aromatic species (i.e., toluene, o-xylene, m + p-xylenes), and larger alkanes (i.e., 2-methylheptane and 2,2,4-trimethylpentane), consistent with tail pipe or gasoline evaporative emissions [*Fraser et al*., 1998; *Gentner et al*., 2009; *Gentner et al*., 2013]. Two well-known markers for combustion engine emissions are NO_x [*Baudic et al*., 2016; *Pierson et al*., 1990] and CO [*Baudic et al*., 2016; *Fraser et al*., 1998; *Pierson et al*., 1990]. Correlations between both of these markers and the PMF traffic factor are stronger in the spring (r^2 of 0.61) than in the summer (r^2 of 0.37–0.38). These relatively weak summer correlations may be a result of differences in photochemical lifetimes: NO_x is short lived, with a typical lifetime of 10 h for an [OH] of 1×10^6 molecules cm^{-3}, in contrast to the 77 day lifetime of CO. The key traffic VOCs have lifetimes on the order of 13 days (ethyne), 20 h (o-xylene), and 49 h (toluene). Thus, in the summer, we expect stronger photochemistry and weaker correlations between NO_x, CO, and the traffic VOCs. To this end, we find that NO_x and CO have a correlation coefficient of 0.73 in spring and 0.51 in summer (Figure S8).

The fourth PMF factor, background, was comprised of longer-lived VOCs with average lifetimes up to 116 days with respect to oxidation by OH under typical summertime conditions (1×10^6 molecules cm^{-3} [OH]), and shorter-lived acetaldehyde and cis-2-butene. This factor also included two chlorofluorcarbons (CFC-11 and CFC-113) with atmospheric lifetimes of 54 and 109 years, respectively [*Rigby et al*., 2013]. This factor represents observed species with local, regional and/or global sources. Because of their long lifetimes, these background VOCs show little diel variability (Figure S9). This factor is dominated by halocarbons, which are typically emitted from industrial sources including degreasing agents and dry cleaning solvents (C_2Cl_4) [*Simpson et al*., 2004], paint stripping (CH_2Cl_2) [*McCulloch and Midgley*, 1996], drinking water and wastewater treatment ($CHCl_3$) [*McCulloch*, 2003], and phased out refrigerants and propellants (CFC-11 and CFC-113) [*Martinerie et al*., 2009]. These halocarbons are ubiquitous in the atmosphere and contribute to the destruction of stratospheric ozone [*Martinerie et al*., 2009; *Seinfeld*, 2016]. Ethyne and benzene, with summertime lifetimes of approximately 46 and 9 days, respectively, are also present in the Background factor. Acetone and acetaldehyde have very different lifetimes, 68 days and 19 h, respectively, against OH oxidation, but both had average mixing ratios >1 ppbv (acetone) and >2 ppbv (acetaldehyde) throughout the day for spring and summer indicating significant background mixing ratios that were captured by the PMF analysis (Figure S11).

The diel profile of the fifth factor, secondary (Figures 2d and 2f), had a pronounced afternoon rise (12:00–4:00 pm) consistent with photochemically driven production on timescales similar to the photochemical production of PAN. PAN, a tracer for secondary or multigenerational chemistry [*Altshuller*, 1993], is well correlated with the secondary factor (r^2 of 0.62 and 0.59 for spring and summer). The main contributors to this secondary factor are short-chain alkyl nitrates and oxidized hydrocarbons including acetone, acetaldehyde, and methyl ethyl ketone (MEK). In urban areas, small-chain monofunctional alkyl nitrates, acetaldehyde, and PAN are dominantly produced by oxidation of primary anthropogenic emissions [e.g., *Flocke et al*., 1998; *Russo et al*., 2010a; *Seinfeld*, 2016; *Sommariva et al*., 2011], while acetone and MEK have primary and secondary anthropogenic sources [*Fischer et al*., 2012; *Yañez-Serrano et al*., 2016].

Of the three measured OVOCs, MEK is the single largest OVOC contributor to the secondary factor, although the correlation between MEK and the secondary factor suggests that the secondary source accounts for 38% of the MEK mixing ratios. This is more than double the percentage reported by *De Gouw et al*. [2005] for secondary anthropogenic production of MEK in New England urban areas. Furthermore, *Sommariva et al*. [2011] modeled the major photochemical production pathways for OVOCs, including MEK, in New England using VOC data from the 2002 New England Air Quality Study [*De Gouw et al*., 2005; *Goldan et al*., 2004] and found n-butane to be the dominant source of MEK (20–30%). The MEK yield from n-butane oxidation is on the order of 80% [*Singh et al*., 2004]. n-Butane is higher in the NFRMA (summer average = 2 ppbv) relative to New York

(0.760 ppbv) and Boston (0.190 ppbv) [*Baker et al*., 2008], indicating that photochemical oxidation of n-butane is likely a major source of MEK in the NFRMA. This implies that ONG activities in the region influence both primary VOC mixing ratios and the atmospheric oxidation chemistry in the region. Acetaldehyde is only weakly correlated with the secondary factor, and this factor makes a small contribution to acetaldehyde (<9%) in the spring. In summer, the secondary factor explains 34% of the observed acetaldehyde mixing ratios.

PMF inherently groups compounds for which the timescale of production and loss are similar [*Yuan et al*., 2012]. This causes VOCs that are photochemically produced or removed on different (slower or faster) timescales than the identified factors to be excluded. The secondary factor is dominated by 2-butyl nitrate, 2-pentyl nitrate, and 3-pentyl nitrate with smaller contributions from ethyl nitrate and propyl nitrates. Alkyl nitrates are formed from the reaction of an alkyl peroxy radical (RO_2) with NO [*Roberts*, 1990]. Hydrogen atom abstraction from a parent alkane by OH is typically the rate limiting step in RO_2 formation [*Seinfeld*, 2016], and we can compare rate constants (k_{OH+VOC}) of those parent alkanes with the formation pathway of OVOCs and PAN. n-Butyl nitrate is formed almost exclusively from the oxidation of n-butane, and the pentyl nitrates from i-pentane and n-pentane; rate constants with OH for these parent hydrocarbons are $(2.36–3.9) \times 10^{-12}$ cm^3 molecule^{-1} s^1 [*Sommariva et al*., 2008]. As described above, the oxidation of n-butane is also a primary pathway for MEK production [*Singh et al*., 2004], demonstrating that timescales for secondary formation of MEK and C_4-C_5 nitrates are similar. Timescales for loss by OH reaction with MEK and C_4-C_5 alkyl nitrates are also similar: both are primarily removed by OH (τ_{OH} = 7–13.5 days for the alkyl nitrates; τ_{OH} = 5.4 days for MEK) [*Chew and Atkinson*, 1996; *Simpson et al*., 2006; *Yañez-Serrano et al*., 2016]. While the photochemical sources of acetone and acetaldehyde are dominated by OH oxidation of propane and ethane, respectively, the lifetimes of these two compounds are quite different (0.8 days for acetaldehyde; 14 days for acetone [*Fischer et al*., 2014]). *Sommariva et al*. [2011] found that acetone and acetaldehyde are predominately formed from OH oxidation of propane and ethane in urban airsheds in New England. Considering the elevated mixing ratios of ethane and propane in the NFRMA versus values reported by [*Baker et al*., 2008] for those New England urban areas, this conclusion is likely also true for the NFRMA. This discrepancy may explain the relatively low correlations of the two OVOCs with the secondary factor.

While isoprene was below the LOD in the spring, an additional PMF factor was identified in the summer that was almost exclusively comprised of isoprene (Figure 2f). Isoprene is the globally dominant biogenic VOC [*Fuentes et al*., 2000; *Kesselmeier and Staudt*, 1999] with a light- and temperature-dependent emission rate. Isoprene is emitted from many broadleaf plants, including spruce, sycamore, poplar, oak, and multiple crops [*Guenther*, 2006; *Guenther et al*., 1994]. The diel profile and temperature dependence (Figure S10) is consistent with an exclusively biogenic source of isoprene in the NFRMA. Isoprene is suppressed in the midafternoon during the sunlight maxima, likely due to a combination of removal by reaction with OH ($k_{OH,isoprene} = 1 \times 10^{-10}$ cm^3 molecule^{-1} s^{-1}), and an expanding afternoon boundary layer. While monoterpenes are emitted by the pine trees that dominate the Rocky Mountains and can be measured by the GC system described herein (LODs of 1–2 pptv); none were observed above the LOD in this 2015 campaign. We hypothesize that the lack of observed monoterpenes was due to their rapid oxidation by O_3 and OH before airmasses reached BAO. We note that substantial urban development has occurred in the Front Range in the last three decades, often accompanied by planting of urban trees. Several common native species, including aspen, oak, and spruce, are moderate to major isoprene emitters [*Guenther et al*., 1994] and common isoprene-emitting urban trees in the NFRMA include oaks, poplars, and willows [*Guenther et al*., 1994; *McHale et al*., 2009].

3.3. PMF Reconstructions of Measured VOCs

The PMF factors and their time series were used to reconstruct the mixing ratio of each VOC (Figure 4 and Table S2). The difference between the "reconstructed" and "observed" VOC mixing ratios can be attributed to the residual—i.e., components that are not captured by the PMF solution. The lack of a suitable reconstruction for some species (i.e., OVOCs) indicates that the sources were not fully captured by PMF, potentially due to the lack of covariability in the data set or to the difficulty in capturing chemical processes that occur on multiple timescales. The C_2-C_8 alkanes, with the exceptions of ethane, the pentane isomers, and n-octane, were well captured by both spring and summer PMF solutions. The PMF reconstruction captured >80% of the mass as defined by the slope of reconstruction versus observation, and >80% of the variance, as

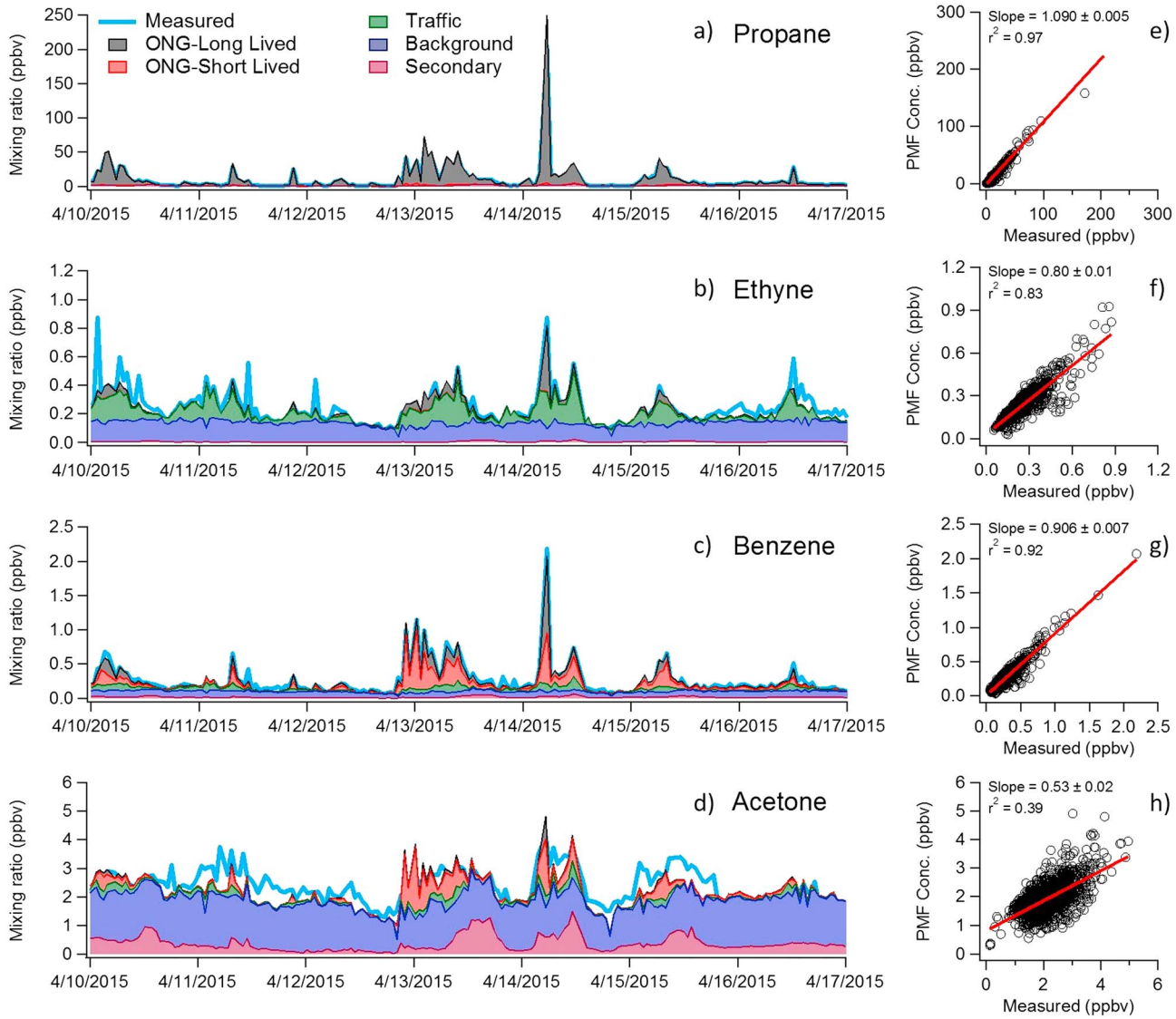

Figure 4. The observed mixing ratios (light blue line) and PMF reconstructions (shaded regions: ONG-long lived, grey; ONG-short lived, red; traffic, dark green; background, blue; and secondary, magenta) of four VOC species for one week (10 April to 17 April 2015) demonstrate the PMF-derived sources of each VOC. For example, the contribution of the ONG-long lived factor (Figure 4a; black shading) to the observed propane concentration is calculated from the product of the ONG-long lived time series (Figures S5 and S6) and the ONG-long lived fractional contribution from propane (0.12 ± 0.03; Figure 2a). Each factor has a positive nonzero contribution to every species, and the full reconstruction of a given species is the sum of the reconstructions from each factor. The correlations between full reconstructions and the measured concentrations vary from species to species. Propane is (e) fully reconstructed and (a) almost entirely attributed to the ONG-long lived factor. Ethyne is (b) dominated by the background and traffic factors but (f) incompletely reconstructed, while benzene has (c, g) contributions from ONG, traffic, and background factors. Acetone (d) has large contributions from both the background and secondary factors but (h) was only partially reconstructed indicating sources that were not captured by the PMF analysis.

defined by the correlation coefficients (Table S2). Benzene and toluene were also well reconstructed. The ONG factors accounted for 74% and 71% of measured benzene for spring and summer, respectively, indicating that traffic is a minor source of benzene in the NFRMA. Toluene was more evenly split between ONG and traffic factors, with 30% from ONG factors and 38% from traffic in spring and 41% from ONG factors and 48% from traffic in the summer. Acetone, acetaldehyde and MEK were associated with the background and secondary factors but contained large residual components that were not captured by the PMF solution (<55% of the mass and variance), suggesting that secondary sources operated on timescales that were quite different from the bulk of the secondary factor or that primary emissions (e.g., solvent use) were not captured by the PMF solution. Similar to the oxygenated organic compounds, the

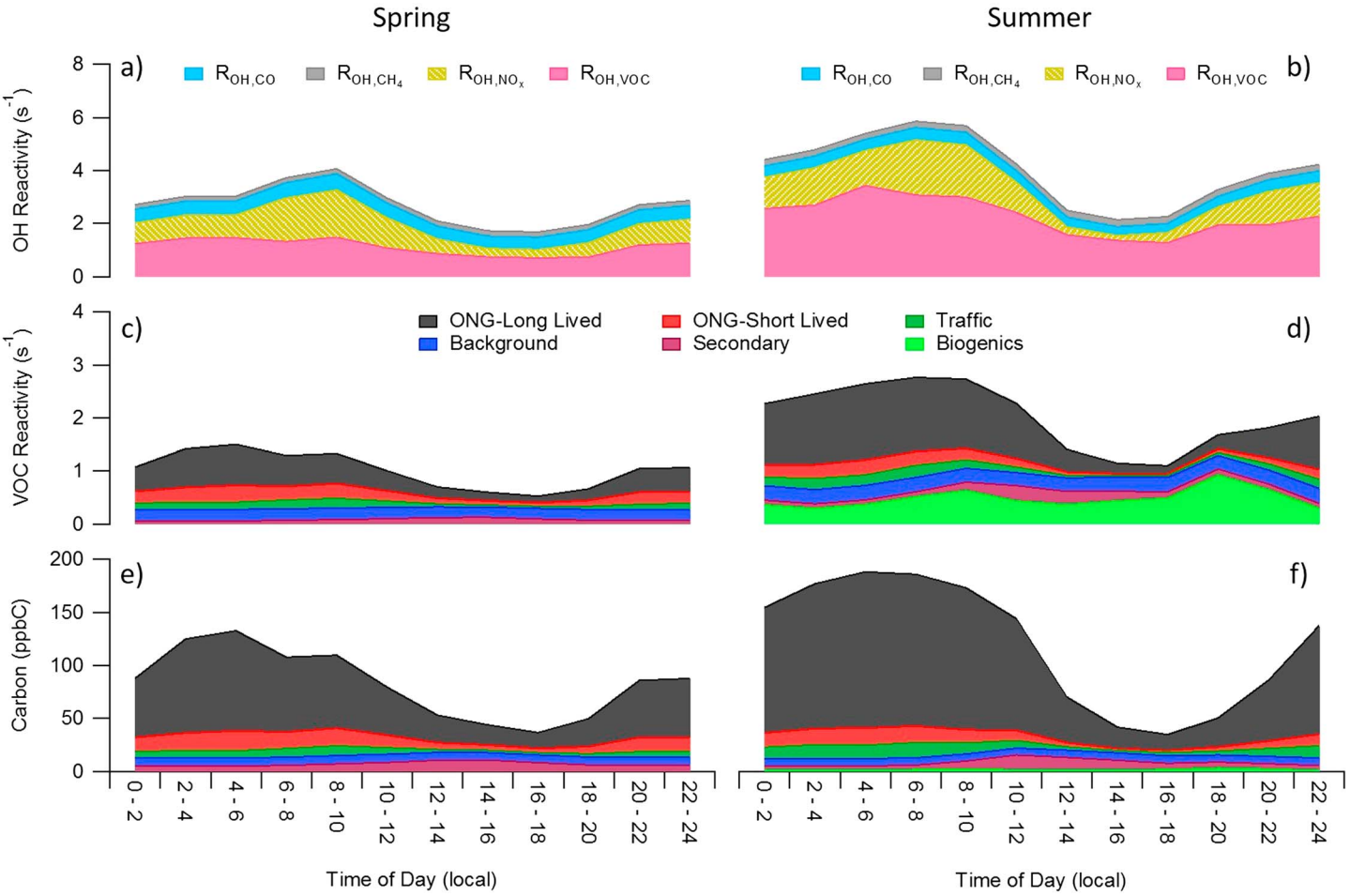

Figure 5. (a, b) Diel cycles of calculated OH Reactivity from equations 1–3 for the spring (Figures 5a, 5c, and 5e) and summer (Figures 5b, 5d, and 5f). Each major contributor to total calculated OH reactivity (Figures 5a and 5b) (VOCs, NO_x, CO, or CH_4) is shown stacked in a separate color. The contributions from each PMF factor to the calculated (c, d) VOC reactivity and (e, f) calculated carbon mixing ratio as a diel cycle. The concentration of each species was reconstructed from PMF factors to determine the VOC reactivity contribution of each species for each factor and thus total VOC reactivity.

halogenated organic species were poorly reconstructed (<58% of the mass), consistent with either local primary emission sources or incomplete capture of the background.

3.4. Organic Carbon Mass and VOC Reactivity

Figures 5 and S12 summarize the relative contributions from NO_x, CH_4, CO, and VOCs on the total calculated OH reactivity (Figures 5a and 5b). The average calculated total OH reactivity was 2.7 and 4.0 s^{-1} in the spring and summer, respectively, with NO_x dominating in the morning (44%, 1.8 s^{-1} in the spring; 36%, 2.1 s^{-1} in the summer). However, observed VOCs dominated the afternoon total calculated OH reactivity (0.7–1.1 s^{-1} in the spring; 1.3–2.4 s^{-1} in the summer). VOCs contributed more OH reactivity in the summer (50–64%) than in the spring (35–48%), resulting from the relative enhancement of biogenics and the evaporative emission of anthropogenic hydrocarbons (section 3.2.). VOCs are a major OH sink in both spring and summer and provide carbon reactivity to initiate the HO_x catalytic cycle from which O_3 is produced. To better understand how different sources affect gas phase organic carbon and VOC reactivity, we investigated the contribution of each PMF factor to total calculated VOC reactivity and total observed organic carbon (Figures 5c–5f). Total observed organic carbon (excluding methane) averaged 100 and 150 ppbC in the spring and summer, respectively, while total observed VOC reactivity (excluding methane) averaged 1.2 and 2.4 s^{-1}. The PMF factors reconstructed >84% of the total observed organic carbon mixing ratio and observed VOC reactivity, accounting for >93% of the variance. The total observed organic carbon mixing ratio was dominated by the ONG factors, which collectively accounted for 43–72% of ppbC in the spring, and 39–76% of ppbC in the

summer. The ONG factors also accounted for the bulk of the morning VOC reactivity in the spring (52–66% of the VOC reactivity), with additional contributions from the background/long-lived factor in the late afternoon (4–6 P.M.). In contrast, the summer VOC reactivity was dominated by the ONG factors only in the morning (46–58% of the reactivity). Despite accounting for <6% of the observed organic carbon mixing ratio during the day, the biogenic factor dominated VOC reactivity in the afternoon (up to 49% of the reactivity between 2 and 6 P.M.) when O_3 mixing ratios were at their peak.

The morning domination of VOC reactivity by ONG sources is consistent with previous results at the same site, 55 ± 18% [*Gilman et al*., 2013] and 52% [*Swarthout et al*., 2013] in February 2011 and 50% in summer 2014 [*McDuffie et al*., 2016]. However, the strong contribution of biogenic VOCs to VOC reactivity is in contrast to a previous study. *McDuffie et al*. [2016] reported that isoprene and monoterpenes contributed only ~8% to total VOC reactivity in the summer of 2012. We hypothesize that the discrepancy is the result of varying biogenic emissions from different drought conditions between the two summers. Temperature distributions for the identical time periods in each year are very similar (Figure S13). Summer 2012 has a larger percentage of winds coming from the west, while summer 2015 has a higher percentage coming from the south (Figure S14). In summer 2015 samples with wind directions from the west had slightly enhanced isoprene mixing ratios. Thus, even with less favorable wind directions for enhanced isoprene, summer 2015 still had significantly elevated mixing ratios.

During the summer of 2012, 33% of the contiguous U.S. was in severe to extreme drought, and 55% of the U.S. was in moderate to extreme drought [*NOAA*, 2012]. In particular, Colorado was in a severe to exceptional drought through July and August 2012 [*NOAA*, 2015]. In contrast to the drought conditions experienced in 2012, the majority of Colorado was not in any drought classification during July and August 2015, and there was also excess soil moisture [*NOAA*, 2015]. Likely as a result of the drought conditions, average isoprene mixing ratios in summer 2012 were 0.06 ppbv versus 0.18 ppbv in summer 2015 for 25 July to 12 August for both years. A detailed review of the density of isoprene emitters in the NFRMA and the impact of drought on each species is beyond the scope of this study. However, we note that biogenic isoprene emissions from many plant species decrease with time and eventually cease under prolonged severe drought conditions [*Brilli et al*., 2007; *Fortunati et al*., 2008; *Guenther*, 2006] and that prolonged drought stress increases tree mortality rates [*Park Williams et al*., 2013].

Traffic is a minor source (<13%) of both organic carbon mixing ratio and VOC reactivity throughout the day in both seasons. While ethene and propene are known tail pipe emissions [e.g., *Gentner et al*., 2009; *Gentner et al*., 2013], they were removed from the PMF analyses for both seasons as a result of spring measurement issues. However, their low summer mixing ratios and moderate OH reactivity accounts for < 4% of the calculated VOC reactivity. Acetaldehyde is the single largest VOC contributor to observed VOC reactivity, contributing 25% of the observed VOC reactivity in the spring and 17% in the summer. To put this in perspective, the background and secondary factors, which accounted for the majority of the acetaldehyde, contributed a combined 28–48% and 21–33% of afternoon VOC reactivity in the spring and summer, respectively. In both factors acetone, acetaldehyde, and MEK are the dominant reactive species that contributed to VOC reactivity. These are clearly underestimates of total VOC reactivity; as most oxidized organic species were not measured in this study. In particular, formaldehyde, methyl vinyl ketone and methacrolein typically contribute substantially to VOC reactivity. For example, *Whalley et al*. [2016] reported that formaldehyde alone accounted for 23% of VOC reactivity in London during July–August 2012.

3.5. Comparison of VOC Reactivity to Other Regions

The magnitude of VOC reactivity and the relative contribution to that reactivity from different compounds or classes of compounds obvio varies across regions. Comparisons of VOC reactivity are difficult because of the varying number of VOCs measured across different campaigns and regions, as well as the reported VOC reactivity statistics (daytime versus full day analyses; median versus average values). However, trends in reactivity have emerged from an array of urban areas, and qualitative comparisons of the similarities and differences between regions can be made and compared to the BAO site.

1. Emissions of alkenes, aromatics, and alkynes from motor vehicle emissions or industrial/petrochemical processes tend to dominate anthropogenic VOC reactivity in urban regions. For example, *Borbon et al*. [2013] reported that aromatics and alkenes from motor vehicle emissions accounted for an average of

50% of calculated VOC reactivity during the CalNex campaign in Pasadena, CA. Similarly, *Gilman et al*. [2009] reported that C_2-C_6 alkenes and aromatics from motor vehicles and petrochemical refinery emissions were responsible for 42% (3.19 s^{-1}) of the 7.5 s^{-1} total calculated VOC reactivity in the Houston/Galveston Bay region. In contrast, we observed little contribution of traffic-related VOCs to the overall VOC reactivity (3–13%) and instead find that ONG activity dominates the anthropogenic reactivity (17–66% of calculated VOC reactivity). However, the total observed VOC reactivity at the BAO site was substantially smaller in both the spring (1.2 s^{-1}) and summer (2.4 s^{-1}) relative to other urban sites.

2. Urban areas in close proximity to forested regions (the eastern U.S. [e.g., *Chameides et al*., 1988; *Millet et al*., 2005; *Warneke et al*., 2004]; and the San Joaquin Valley, CA [*Pusede et al*., 2014]) can have significant contributions from biogenic VOCs and their oxidation products to total VOC reactivity. These biogenic sources can dominate VOC reactivity during the daytime. From VOC measurements made in Pittsburgh, PA, in summer 2002, *Millet et al*. [2005] reported a median daytime VOC reactivity of 6.72 s^{-1} of which 70% (4.71 s^{-1}) was attributed to isoprene and isoprene oxidation products. Our observations suggest that biogenic VOCs were important contributors to VOC reactivity (up to 47%) in summer 2015, even though the absolute magnitude of the biogenic contribution at BAO (0.29–0.93 s^{-1}) was far smaller than most other biogenic-influenced urban sites.
3. OVOCs from primary urban emissions, oxidation of primary anthropogenic emissions, or oxidation of biogenic emissions can be major contributors to urban VOC reactivity [e.g., *Borbon et al*., 2013; *Gilman et al*., 2009; *Millet et al*., 2005; *Swarthout et al*., 2015] and can actually dominant VOC reactivity in some cities. Based on VOC measurements in London (July–August 2012), *Whalley et al*. [2016] reported that OVOCs excluding alcohols, but including formaldehyde, acetaldehyde, and isoprene oxidation products contributed 62% (3.45 s^{-1}) of the total calculated VOC reactivity of 5.54 s^{-1}. Unfortunately, our data set is inadequate for extensively investigating the role of OVOCs to total VOC reactivity at BAO.

As noted by *McDuffie et al*. [2016], few studies have evaluated the impact of VOCs from ONG operations on regional summertime O_3 production, especially in urban regions. However, it is clear from the analysis above that VOC reactivity at BAO is quite different from other well-studied urban areas and is more similar to semi-rural areas in close proximity to natural gas operations (e.g., Hickory site, Pennsylvania [*Swarthout et al*., 2015]). The total calculated summer VOC reactivity of 2.4 s^{-1} in the NFRMA (excluding CH_4 and including biogenics) is much lower than urban areas detailed above, even when differences in VOC measurement suites are considered but is similar to the value of 3.1 s^{-1} reported at the Hickory site [*Swarthout et al*., 2015]. As discussed above, the NFRMA VOC composition in 2015 was predominantly ONG related C_2-C_6 alkanes and minimally impacted by traffic-related alkenes and aromatics. This contrasts with most other urban regions, in which traffic is typically the dominant anthropogenic VOC source. During summer 2015, biogenic VOCs (isoprene) impacted total VOC reactivity at BAO, accounting for an average of 20%, and up to 49%, of the total calculated VOC reactivity. These fractional contributions of biogenic VOC reactivity to total reactivity were much higher than Pasadena (<2%) [*Borbon et al*., 2013] and Houston (7%) [*Gilman et al*., 2009], but lower than Pittsburgh (70%) [*Millet et al*., 2005].

4. Conclusions

The spring and summer 2015 VOC data set provides an updated long-term multiseason VOC measurement suite for the NFRMA that can be compared to previous measurements and will be used to investigate O_3 production in the NFRMA. Using PMF source attribution, we found that unlike most urban regions, traffic-related VOCs were minor contributors to reactivity. Instead, ONG sources contributed substantially to organic carbon mixing ratios and VOC reactivity and remain obvious targets for VOC emissions control. Oxygenated VOCs from direct emissions or secondary production are a major OH radical sink. The enhanced isoprene contribution in the summer of 2015 relative to drought-stricken 2012 suggests that biogenic hydrocarbons from agriculture and urban trees have the potential to impact regional air quality and may be strongly affected by drought stress [*Dai*, 2013]. Future drought-driven changes in biogenic VOCs have the potential to suppress VOC reactivity in the NFRMA [*Brilli et al*., 2007; *Fortunati et al*., 2008; *Guenther et al*., 1996; *Park Williams et al*., 2013]. Despite their large contributions to VOC reactivity, the sources of OVOCs in the NFRMA (acetone, acetaldehyde, and MEK) remain the least constrained of the measured VOC suite. PMF reconstructions of these species were poor, and future work characterizing the oxidized organic compounds and their chemistry are essential for constraining the OH reactivity and radical budget of the NFRMA region.

Acknowledgments

We acknowledge the National Oceanic and Atmospheric Administration for funding (award NA14OAR4310148). We thank Jessica Gilman and Brian Lerner for comparison of standards and helpful advice on VOC sampling and Dan Wolfe, Bruce Bartram, and Gerhard Hubler for support at the BAO site. We acknowledge Sam Hall of NCAR for NO_2 photolysis rate data from 2014, which was included in Figure S10. The data used in this manuscript can be found in Tables 1 and S1 and in a repository hosted by the National Oceanic and Atmospheric Administration (http://esrl.noaa.gov/csd/groups/csd7/measurements/2015songnex/).

References

Altshuller, A. (1993), PANs in the atmosphere, *Air Waste*, *43*(9), 1221–1230.

Atkinson, R. (1986), Kinetics and mechanisms of the gas-phase reactions of the hydroxyl radical with organic compounds under atmospheric conditions, *Chem. Rev.*, *86*(1), 69–201.

Atkinson, R., et al. (2001), Summary of evaluated kinetic and photochemical data for atmospheric chemistry, *Not in System*, 1–56.

Atkinson, R., and J. Arey (2003), Atmospheric degradation of volatile organic compounds, *Chem. Rev.*, *103*(12), 4605–4638.

Baker, A. K., A. K. Baker, A. J. Beyersdorf, L. A. Doezema, A. Katzenstein, S. Meinardi, I. J. Simpson, D. R. Blake, and F. Sherwood Rowland (2008), Measurements of nonmethane hydrocarbons in 28 United States cities, *Atmos. Environ.*, *42*(1), 170–182.

Baudic, A., et al. (2016), Seasonal variability and source apportionment of volatile organic compounds (VOCs) in the Paris megacity (France), *Atmos. Chem. Phys.*, *16*(18), 11,961–11,989, doi:10.5194/acp-16-11961-2016.

Berger, B., and K. Anderson (1981), *Modern petroleum: A Basic Primer of the Industry*, pp. 255, PennWell Books, Tulsa, Okla.

Bon, D. M., et al. (2011), Measurements of volatile organic compounds at a suburban ground site (T1) in Mexico City during the MILAGRO 2006 campaign: Measurement comparison, emission ratios, and source attribution, *Atmos. Chem. Phys.*, *11*(6), 2399–2421, doi:10.5194/acp-11-2399-2011.

Borbon, A., et al. (2013), Emission ratios of anthropogenic volatile organic compounds in northern mid-latitude megacities: Observations versus emission inventories in Los Angeles and Paris, *J. Geophys. Res. Atmos.*, *118*, 2041–2057, doi:10.1002/jgrd.50059.

Brilli, F., C. Barta, A. Fortunati, M. Lerdau, F. Loreto, and M. Centritto (2007), Response of isoprene emission and carbon metabolism to drought in white poplar (Populus alba) saplings, *New Phytol.*, *175*(2), 244–254.

Brown, S. S., et al. (2013), Nitrogen, Aerosol Composition, and Halogens on a Tall Tower (NACHTT): Overview of a wintertime air chemistry field study in the front range urban corridor of Colorado, *J. Geophys. Res. Atmos.*, *118*, 8067–8085, doi:10.1002/jgrd.50537.

Colorado Department of Public Health and Environment (2014), *Control of Ozone Via Ozone Precursors and Control of Hydocarbons Via Oil and Gas Emissions*, Colorado Department of Public Health and Environment, Denver, Colo.

Chameides, W., R. Lindsay, J. Richardson, and C. Kiang (1988), The role of biogenic hydrocarbons in urban photochemical smog: Atlanta as a case study, *Science*, *241*(4872), 1473–1475.

Chatani, S., et al. (2009), Sensitivity analyses of OH missing sinks over Tokyo metropolitan area in the summer of 2007, *Atmos. Chem. Phys.*, *9*(22), 8975–8986.

Chew, A. A., and R. Atkinson (1996), OH radical formation yields from the gas-phase reactions of O_3 with alkenes and monoterpenes, *J. Geophys. Res.*, *101*(D22), 28,649–28,653, doi:10.1029/96JD02722.

Dai, A. (2013), Increasing drought under global warming in observations and models, *Nat. Clim. Change*, *3*(1), 52–58. [Available at http://www.nature.com/nclimate/journal/v3/n1/abs/nclimate1633.html#supplementary-information.]

De Gouw, J., et al. (2005), Budget of organic carbon in a polluted atmosphere: Results from the New England Air Quality Study in 2002, *J. Geophys. Res.*, *110*, D16305, doi:10.1029/2004JD005623.

Di Carlo, P., et al. (2004), Missing OH reactivity in a forest: Evidence for unknown reactive biogenic VOCs, *Science*, *304*(5671), 722–725.

Dolgorouky, C., V. Gros, R. Sarda-Esteve, V. Sinha, J. Williams, N. Marchand, S. Sauvage, L. Poulain, J. Sciare, and B. Bonsang (2012), Total OH reactivity measurements in Paris during the 2010 MEGAPOLI winter campaign, *Atmos. Chem. Phys.*, *12*(20), 9593–9612.

Dominutti, P. A., T. Nogueira, A. Borbon, M. de Fatima Andrade, and A. Fornaro (2016), One-year of NMHCs hourly observations in São Paulo megacity: Meteorological and traffic emissions effects in a large ethanol burning context, *Atmos. Environ.*, *142*, 371–382.

Dusanter, S., et al. (2009), Measurements of OH and HO_2 concentrations during the MCMA-2006 field campaign—Part 2: Model comparison and radical budget, *Atmos. Chem. Phys.*, *9*(18), 6655–6675.

Edwards, P. M., et al. (2013), OH reactivity in a South East Asian tropical rainforest during the oxidant and particle photochemical processes (OP3) project, *Atmos. Chem. Phys.*, *13*(18), 9497–9514.

U.S. Energy Information Administration (EIA) (2016a), Crude oil production. [Available at http://www.eia.gov/dnav/pet/pet_crd_crpdn_adc_mbbl_m.htm,9/30/2016.]

EIA (2016b), Natural gas gross withdrawals and production. [Available at http://www.eia.gov/dnav/ng/ng_prod_sum_a_EPG0_VGM_mmcf_m.htm,9/30/2016.]

EIA (2016c), Number of producing gas wells. [Available at https://www.eia.gov/dnav/ng/ng_prod_wells_s1_a.htm,9/30/2016.]

Environmental Protection Agency (2014), *EPA Positive Matrix Factorization (PMF) 5.0 Fundamentals and User Guide*, Environmental Protection Agency - Office of Research and Development, Washington, D. C.

Farmer, D. et al. (2011), Impact of organic nitrates on urban ozone production, *Atmos. Chem. Phys.*, *11*(9), 4085–4094.

Fischer, E. V., et al. (2014), Atmospheric peroxyacetyl nitrate (PAN): A global budget and source attribution, *Atmos. Chem. Phys.*, *14*(5), 2679–2698, doi:10.5194/acp-14-2679-2014.

Fischer, E., D. J. Jacob, D. Millet, R. M. Yantosca, and J. Mao (2012), The role of the ocean in the global atmospheric budget of acetone, *Geophys. Res. Lett.*, *39*, L01807, doi:10.1029/2011GL050086.

Flocke, F., A. Volz-Thomas, H.-J. Buers, W. Pätz, H.-J. Garthe, and D. Kley (1998), Long-term measurements of alkyl nitrates in southern Germany: 1. General behavior and seasonal and diurnal variation, *J. Geophys. Res.*, *103*(D5), 5729–5746, doi:10.1029/97JD03461.

Flocke, F., A. Weinheimer, A. L. Swanson, J. Roberts, R. Schmitt, and S. Shertz (2005), On the measurement of PANs by gas chromatography and electron capture detection, *J. Atmos. Chem.*, *52*(1), 19–43, doi:10.1007/s10874-005-6772-0.

Fortunati, A., C. Barta, F. Brilli, M. Centritto, I. Zimmer, J. P. Schnitzler, and F. Loreto (2008), Isoprene emission is not temperature-dependent during and after severe drought-stress: A physiological and biochemical analysis, *Plant J.*, *55*(4), 687–697.

Fraser, M. P., G. R. Cass, and B. R. Simoneit (1998), Gas-phase and particle-phase organic compounds emitted from motor vehicle traffic in a Los Angeles roadway tunnel, *Environ. Sci. Technol.*, *32*(14), 2051–2060.

Fuentes, J. D., et al. (2000), Biogenic hydrocarbons in the atmospheric boundary layer: A review, *Bull. Am. Meteorol. Soc.*, *81*(7).

Gentner, D. R., R. A. Harley, A. M. Miller, and A. H. Goldstein (2009), Diurnal and seasonal variability of gasoline-related volatile organic compound emissions in Riverside, California, *Environ. Sci. Technol.*, *43*(12), 4247–4252.

Gentner, D. R., et al. (2013), Chemical composition of gas-phase organic carbon emissions from motor vehicles and implications for ozone production, *Environ. Sci. Technol.*, *47*(20), 11,837–11,848, doi:10.1021/es401470e.

Gilman, J. B., et al. (2009), Measurements of volatile organic compounds during the 2006 TexAQS/GoMACCS campaign: Industrial influences, regional characteristics, and diurnal dependencies of the OH reactivity, *J. Geophys. Res.*, *114*, D00F06, doi:10.1029/2008JD011525.

Gilman, J. B., B. M. Lerner, W. C. Kuster, and J. A. de Gouw (2013), Source signature of volatile organic compounds from oil and natural gas operations in northeastern Colorado, *Environ. Sci. Technol.*, *47*(3), 1297–1305, doi:10.1021/es304119a.

Goldan, P. D., W. C. Kuster, E. Williams, P. C. Murphy, F. C. Fehsenfeld, and J. Meagher (2004), Nonmethane hydrocarbon and oxy hydrocarbon measurements during the 2002 New England Air Quality Study, *J. Geophys. Res.*, *109*, D21309, doi:10.1029/2003JD004455.

Goldstein, A. H. (2007), Known and unexplored organic constituents in the earth's atmosphere, *Environ. Sci. Technol.*, *41*(5), 1514–1521.

Guenther, A. (2006), Estimates of global terrestrial isoprene emissions using MEGAN (Model of Emissions of Gases and Aerosols from Nature), *Atmos. Chem. Phys.*, *6*.

Guenther, A., P. Zimmerman, and M. Wildermuth (1994), Natural volatile organic compound emission rate estimates for US woodland landscapes, *Atmos. Environ.*, *28*(6), 1197–1210.

Guenther, A., P. Zimmerman, L. Klinger, J. Greenberg, C. Ennis, K. Davis, W. Pollock, H. Westberg, G. Allwine, and C. Geron (1996), Estimates of regional natural volatile organic compound fluxes from enclosure and ambient measurements, *J. Geophys. Res.*, *101*(D1), 1345–1359, doi:10.1029/95JD03006.

Guha, A., D. Gentner, R. Weber, R. Provencal, and A. Goldstein (2015), Source apportionment of methane and nitrous oxide in California's San Joaquin Valley at CalNex 2010 via positive matrix factorization, *Atmos. Chem. Phys.*, *15*(20), 12,043–12,063.

Hansen, R., et al. (2014), Measurements of total hydroxyl radical reactivity during CABINEX 2009—Part 1: Field measurements, *Atmos. Chem. Phys.*, *14*(6), 2923–2937.

Helmig, D., et al. (2016), Reversal of global atmospheric ethane and propane trends largely due to US oil and natural gas production, *Nat. Geosci.*, *9*(7), 490–495.

Hopke, P. K. (2000), A guide to positive matrix factorization, paper presented at Workshop on UNMIX and PMF as Applied to PM2.

Karl, T., A. Guenther, C. Spirig, A. Hansel, and R. Fall (2003), Seasonal variation of biogenic VOC emissions above a mixed hardwood forest in northern Michigan, *Geophys. Res. Lett.*, *30*(23), 2186, doi:10.1029/2003GL018432.

Katzenstein, A. S., L. A. Doezema, I. J. Simpson, D. R. Blake, and F. S. Rowland (2003), Extensive regional atmospheric hydrocarbon pollution in the southwestern United States, *Proc. Natl. Acad. Sci. U.S.A.*, *100*(21), 11,975–11,979, doi:10.1073/pnas.1635258100.

Kesselmeier, J., and M. Staudt (1999), Biogenic volatile organic compounds (VOC): An overview on emission, physiology and ecology, *J. Atmos. Chem.*, *33*(1), 23–88, doi:10.1023/a:1006127516791.

Lanz, V., M. R. Alfarra, U. Baltensperger, B. Buchmann, C. Hueglin, and A. Prévôt (2007), Source apportionment of submicron organic aerosols at an urban site by factor analytical modelling of aerosol mass spectra, *Atmos. Chem. Phys.*, *7*(6), 1503–1522.

Lee, E., C. K. Chan, and P. Paatero (1999), Application of positive matrix factorization in source apportionment of particulate pollutants in Hong Kong, *Atmos. Environ.*, *33*(19), 3201–3212.

Martinerie, P., et al. (2009), Long-lived halocarbon trends and budgets from atmospheric chemistry modelling constrained with measurements in polar firn, *Atmos. Chem. Phys.*, *9*(12), 3911–3934.

McCulloch, A. (2003), Chloroform in the environment: occurrence, sources, sinks and effects, *Chemosphere*, *50*(10), 1291–1308.

McCulloch, A., and P. M. Midgley (1996), The production and global distribution of emissions of trichloroethene, tetrachloroethene and dichloromethane over the period 1988–1992, *Atmos. Environ.*, *30*(4), 601–608.

McDuffie, E. E., et al. (2016), Influence of oil and gas emissions on summertime ozone in the Colorado Northern Front Range, *J. Geophys. Res. Atmos.*, *121*, 8712–8729, doi:10.1002/2016JD025265.

McHale, M. R., I. C. Burke, M. A. Lefsky, P. J. Peper, and E. G. McPherson (2009), Urban forest biomass estimates: Is it important to use allometric relationships developed specifically for urban trees?, *Urban Ecosyst.*, *12*(1), 95–113, doi:10.1007/s11252-009-0081-3.

Millet, D. B., N. M. Donahue, S. N. Pandis, A. Polidori, C. O. Stanier, B. J. Turpin, and A. H. Goldstein (2005), Atmospheric volatile organic compound measurements during the Pittsburgh Air Quality Study: Results, interpretation, and quantification of primary and secondary contributions, *J. Geophys. Res.*, *110*, D07S07, doi:10.1029/2004JD004601.

Park Williams. A., et al. (2013), Temperature as a potent driver of regional forest drought stress and tree mortality, *Nat. Clim. Change*, *3*(3), 292–297. [Available at http://www.nature.com/nclimate/journal/v3/n3/abs/nclimate1693.html#supplementary-information.]

NOAA (2012), National centers for environmental information, State of the Climate: Drought for August 2012. [Available at https://www.ncdc.noaa.gov/sotc/drought/201208,9/1/2012.]

NOAA (2015), National centers for environmental information, State of the Climate: Drought for August 2015. [Available at http://www.ncdc.noaa.gov/sotc/drought/201508,9/1/2015.]

Paatero, P. (2000), *User's Guide for Positive Matrix Factorization Programs PMF2 and PMF3*, Univ. Helsinki, Helsinki.

Paatero, P., and U. Tapper (1994), Positive matrix factorization: A non-negative factor model with optimal utilization of error estimates of data values, *Environmetrics*, *5*(2), 111–126.

Pétron, G., et al. (2012), Hydrocarbon emissions characterization in the Colorado Front Range: A pilot study, *J. Geophys. Res.*, *117*, D04304, doi:10.1029/2011JD016360.

Pétron, G., et al. (2014), A new look at methane and nonmethane hydrocarbon emissions from oil and natural gas operations in the Colorado Denver-Julesburg Basin, *J. Geophys. Res. Atmos.*, *119*, 6836–6852, doi:10.1002/2013JD021272.

Piccot, S. D., J. J. Watson, and J. W. Jones (1992), A global inventory of volatile organic compound emissions from anthropogenic sources, *J. Geophys. Res.*, *97*(D9), 9897–9912, doi:10.1029/92JD00682.

Pierson, W. R., A. W. Gertler, and R. L. Bradow (1990), Comparison of the SCAQS tunnel study with other on road vehicle emission data, *J. Air Waste Manage. Assoc.*, *40*(11), 1495–1504.

Pusede, S., et al. (2014), On the temperature dependence of organic reactivity, nitrogen oxides, ozone production, and the impact of emission controls in San Joaquin Valley, California, *Atmos. Chem. Phys.*, *14*(7), 3373–3395.

Rigby, M., et al. (2013), Re-evaluation of the lifetimes of the major CFCs and CH_3CCl_3 using atmospheric trends, *Atmos. Chem. Phys.*, *13*(5), 2691–2702, doi:10.5194/acp-13-2691-2013.

Roberts, J. M. (1990), The atmospheric chemistry of organic nitrates, *Atmos. Environ. Part A*, *24*(2), 243–287.

Rosen, R. S., E. C. Wood, P. J. Wooldridge, J. A. Thornton, D. A. Day, W. Kuster, E. J. Williams, B. T. Jobson, and R. C. Cohen (2004), Observations of total alkyl nitrates during Texas Air Quality Study 2000: Implications for O3 and alkyl nitrate photochemistry, *J. Geophys. Res.*, *109*(D7), D07303, doi:10.1029/2003JD004227.

Russo, R. S., Y. Zhou, K. B. Haase, O. W. Wingenter, E. K. Frinak, H. Mao, R. W. Talbot, and B. C. Sive (2010a), Temporal variability, sources, and sinks of C 1-C 5 alkyl nitrates in coastal New England, *Atmos. Chem. Phys.*, *10*(4), 1865–1883.

Russo, R. S., Y. Zhou, M. L. White, H. Mao, R. Talbot, and B. C. Sive (2010b), Multi-year (2004–2008) record of nonmethane hydrocarbons and halocarbons in New England: Seasonal variations and regional sources, *Atmos. Chem. Phys.*, *10*(10), 4909–4929, doi:10.5194/acp-10-4909-2010.

Sander, S. P., et al. (2015), Chemical kinetics and photochemical data for use in atmospheric studies, evaluation no. 18, Jet Propulsion Laboratory, National Aeronautics and Space Administration, Pasadena, Calif.

Seinfeld, J. H. (2016), *Atmospheric Chemistry and Physics: From Air Pollution To Climate Change*, John Wiley, Hoboken, N. J.

Simpson, I. J., S. Meinardi, N. J. Blake, F. S. Rowland, and D. R. Blake (2004), Long-term decrease in the global atmospheric burden of tetrachloroethene (C2Cl4), *Geophys. Res. Lett.*, *31*, L08108, doi:10.1029/2003GL019351.

Simpson, I. J., T. Wang, H. Guo, Y. H. Kwok, F. Flocke, E. Atlas, S. Meinardi, F. Sherwood Rowland, and D. R. Blake (2006), Long-term atmospheric measurements of C1–C5 alkyl nitrates in the Pearl River Delta region of southeast China, *Atmos. Environ.*, *40*(9), 1619–1632, doi:10.1016/j.atmosenv.2005.10.062.

Singh, H., et al. (2004), Analysis of the atmospheric distribution, sources, and sinks of oxygenated volatile organic chemicals based on measurements over the Pacific during TRACE-P, *J. Geophys. Res.*, *109*, D15S07, doi:10.1029/2003JD003883.

Sive, B. C., Y. Zhou, D. Troop, Y. Wang, W. C. Little, O. W. Wingenter, R. S. Russo, R. K. Varner, and R. Talbot (2005), Development of a cryogen-free concentration system for measurements of volatile organic compounds, *Anal. Chem.*, *77*(21), 6989–6998, doi:10.1021/ac0506231.

Sommariva, R., et al. (2008), A study of organic nitrates formation in an urban plume using a master chemical mechanism, *Atmos. Environ.*, *42*(23), 5771–5786.

Sommariva, R., J. A. De Gouw, M. Trainer, E. Atlas, P. D. Goldan, W. C. Kuster, C. Warneke, and F. C. Fehsenfeld (2011), Emissions and photochemistry of oxygenated VOCs in urban plumes in the northeastern United States, *Atmos. Chem. Phys.*, *11*(14), 7081–7096, doi:10.5194/acp-11-7081-2011.

Song, Y., Y. Zhang, S. Xie, L. Zeng, M. Zheng, L. G. Salmon, M. Shao, and S. Slanina (2006), Source apportionment of PM2. 5 in Beijing by positive matrix factorization, *Atmos. Environ.*, *40*(8), 1526–1537.

Swarthout, R. F. (2014), *Organic Compound Emissions from Unconventional Natural Gas Production: Source Signatures and Air Quality Impacts*, Univ. of New Hampshire, Durham, N. H.

Swarthout, R. F., R. S. Russo, Y. Zhou, A. H. Hart, and B. C. Sive (2013), Volatile organic compound distributions during the NACHTT campaign at the Boulder Atmospheric Observatory: Influence of urban and natural gas sources, *J. Geophys. Res. Atmos.*, *118*, 10,614–10,637, doi:10.1002/jgrd.50722.

Swarthout, R. F., R. S. Russo, Y. Zhou, B. M. Miller, B. Mitchell, E. Horsman, E. Lipsky, D. C. McCabe, E. Baum, and B. C. Sive (2015), Impact of Marcellus Shale natural gas development in southwest Pennsylvania on volatile organic compound emissions and regional air quality, *Environ. Sci. Technol.*, *49*(5), 3175–3184, doi:10.1021/es504315f.

Thompson, C. R., J. Hueber, and D. Helmig (2014), Influence of oil and gas emissions on ambient atmospheric non-methane hydrocarbons in residential areas of northeastern Colorado, *Elem. Sci. Anth.*, *2*, 000035, doi:10.12952/journal.elementa.000035.

U.S.-Census (2016), Quick facts—Colorado. [Available at http://www.census.gov/quickfacts/table/PST045215/08,00,2015.]

Ulbrich, I., M. Canagaratna, Q. Zhang, D. Worsnop, and J. Jimenez (2009), Interpretation of organic components from positive matrix factorization of aerosol mass spectrometric data, *Atmos. Chem. Phys.*, *9*(9), 2891–2918.

Warneke, C., et al. (2004), Comparison of daytime and nighttime oxidation of biogenic and anthropogenic VOCs along the New England coast in summer during New England Air Quality Study 2002, *J. Geophys. Res.*, *109*, D10309, doi:10.1029/2003JD004424.

Warneke, C., et al. (2014), Volatile organic compound emissions from the oil and natural gas industry in the Uinta Basin, Utah: Point sources compared to ambient air composition, *Atmos. Chem. Phys. Discuss.*, *14*, 11,895–11,927.

Watson, J. G., J. C. Chow, and E. M. Fujita (2001), Review of volatile organic compound source apportionment by chemical mass balance, *Atmos. Environ.*, *35*(9), 1567–1584.

Whalley, L., D. Stone, B. Bandy, R. Dunmore, J. F. Hamilton, J. Hopkins, J. D. Lee, A. C. Lewis, and D. E. Heard (2016), Atmospheric OH reactivity in central London: Observations, model predictions and estimates of in situ ozone production, *Atmos. Chem. Phys.*, *16*(4), 2109–2122.

Williams, B., A. H. Goldstein, N. M. Kreisberg, S. V. Hering, D. R. Worsnop, I. M. Ulbrich, K. S. Docherty, and J. L. Jimenez (2010), Major components of atmospheric organic aerosol in southern California as determined by hourly measurements of source marker compounds, *Atmos. Chem. Phys.*, *10*(23), 11,577–11,603.

Yañez-Serrano, A.-M., et al. (2016), Atmospheric mixing ratios of methyl ethyl ketone (2-butanone) in tropical, boreal, temperate and marine environments, *Atmos. Chem. Phys. Discuss.*, *16*(17), 10,965–10,984.

Yuan, B., et al. (2012), Volatile organic compounds (VOCs) in urban air: How chemistry affects the interpretation of positive matrix factorization (PMF) analysis, *J. Geophys. Res.*, *117*, D24302, doi:10.1029/2012JD018236.

Zhou, Y., R. K. Varner, R. S. Russo, O. W. Wingenter, K. B. Haase, R. Talbot, and B. C. Sive (2005), Coastal water source of short-lived halocarbons in New England, *J. Geophys. Res.*, *110*, D21302, doi:10.1029/2004JD005603.

Zhou, Y., H. Mao, R. S. Russo, D. R. Blake, O. W. Wingenter, K. B. Haase, J. Ambrose, R. K. Varner, R. Talbot, and B. C. Sive (2008), Bromoform and dibromomethane measurements in the seacoast region of New Hampshire, 2002–2004, *J. Geophys. Res.*, *113*, D08305, doi:10.1029/2007JD009103.